Modeling non-equilibrium mass transport in biologically reactive porous media.

Yohan Davit, Gerald Debenest, Brian D. Wood, Michel Quintard

Modeling non-equilibrium mass transport in biologically reactive porous media

Yohan Davit [a,c,*], Gérald Debenest [a,b], Brian D. Wood [d], Michel Quintard [a,b]

[a] Université de Toulouse; INPT, UPS; IMFT (Institut de Mécanique des Fluides de Toulouse) Allée Camille Soula F-31400 Toulouse, France
[b] CNRS; IMFT F-31400 Toulouse, France
[c] Université de Toulouse; INPT, UPS; ECOLAB Rue Jeanne Marvig F-31055 Toulouse, France
[d] School of Chemical, Biological, and Environmental Engineering, Oregon State University, Corvallis, OR 97331, United States

Keywords:
Porous media
Biofilms
Upscaling
Volume averaging
Non-equilibrium
One-equation model

A B S T R A C T

We develop a one-equation non-equilibrium model to describe the Darcy-scale transport of a solute undergoing biodegradation in porous media. Most of the mathematical models that describe the macroscale transport in such systems have been developed intuitively on the basis of simple conceptual schemes. There are two problems with such a heuristic analysis. First, it is unclear how much information these models are able to capture; that is, it is not clear what the model's domain of validity is. Second, there is no obvious connection between the macroscale effective parameters and the microscopic processes and parameters. As an alternative, a number of upscaling techniques have been developed to derive the appropriate macroscale equations that are used to describe mass transport and reactions in multiphase media. These approaches have been adapted to the problem of biodegradation in porous media with biofilms, but most of the work has focused on systems that are restricted to small concentration gradients at the microscale. This assumption, referred to as the *local mass equilibrium* approximation, generally has constraints that are overly restrictive. In this article, we devise a model that does not require the assumption of local mass equilibrium to be valid. In this approach, one instead requires only that, at sufficiently long times, anomalous behaviors of the third and higher spatial moments can be neglected; this, in turn, implies that the macroscopic model is well represented by a convection–dispersion–reaction type equation. This strategy is very much in the spirit of the developments for Taylor dispersion presented by Aris (1956). On the basis of our numerical results, we carefully describe the domain of validity of the model and show that the *time-asymptotic constraint* may be adhered to even for systems that are not at local mass equilibrium.

1. Introduction

Biodegradation in porous media has been the subject of extensive studies from the environmental engineering point of view [1–5]. Reactions are mediated by microorganisms (primarily bacteria, fungi, archaea, and protists, although others may be present) aggregated and coated within an extracellular polymeric matrix; together, these which form are generically called biofilms. There has been significant interest for their role in bioremediation of soils and subsurfaces [6–12] and, more recently, for their application to supercritical CO_2 storage [13,14]. Numerous models for describing the transport of solutes, such as organic contaminants or injected nutrients, through geological formations as illustrated in Fig. 1, have been developed. Reviews of these mathematical and physical representations of biofilms processes can be found in [15] and [16].

* Corresponding author. Université de Toulouse; INPT, UPS; IMFT (Institut de Mécanique des Fluides de Toulouse) Allée Camille Soula F-31400 Toulouse, France.
E-mail addresses: davit@cict.fr (Y. Davit), debenest@imft.fr (G. Debenest), brian.wood@oregonstate.edu (B.D. Wood), quintard@imft.fr (M. Quintard).

1.1. One-equation local mass equilibrium model

In many applications, the macroscopic balance laws for mass transport in such hierarchical porous media with biofilms have been elaborated by inspection. For example, the advection–dispersion–reaction type Eq. (1) is commonly considered to describe the Darcy-scale transport of a contaminant/nutrient represented by a concentration $\langle c_\gamma \rangle^\gamma$ in the water γ-phase. Brackets notations are here as a reminder that this concentration must be defined in some averaged sense.

$$\frac{\partial \langle c_\gamma \rangle^\gamma}{\partial t} + \langle \mathbf{v}_\gamma \rangle^\gamma \cdot \nabla \langle c_\gamma \rangle^\gamma = \nabla \cdot \left(\mathbf{D} \cdot \nabla \langle c_\gamma \rangle^\gamma \right) + \mathcal{R} \tag{1}$$

In this expression, $\langle \mathbf{v}_\gamma \rangle^\gamma$ is the groundwater velocity and $\mathbf{D}$ is a dispersion tensor. The reaction rate $\mathcal{R}$ is usually assumed to have a Monod form $\mathcal{R} = -\alpha \frac{\langle c_\gamma \rangle^\gamma}{\langle c_\gamma \rangle^\gamma + \mathcal{K}}$, where α and $\mathcal{K}$ are parameters (discussed in Section 3.5). It is common to assume that the solute transport can be uncoupled from the growth process [17,18], that is, to consider that the characteristic times for these two processes are

Nomenclature

Roman symbols

$\mathbf{b}_i$	Closure parameter in the i-phase associated to $\nabla\langle c\rangle^{\gamma\omega}$, (m).
$\mathbf{b}_i'$	Closure parameter in the i-phase associated to $\nabla\langle c\rangle^{\gamma\omega}$ normalized to l_γ, (−).
c_i	Pointwise substrate concentration in the i-phase, (mol m^{-3}).
c_i'	Pointwise substrate concentration in the i-phase normalized with c_0, (−).
c_0	Substrate input concentration, (mol m^{-3}).
$\langle C\rangle$	Generalized spatial average of c_i, (mol m^{-3}).
$\langle c_i\rangle$	Superficial spatial average of c_i, (mol m^{-3}).
$\langle c_i\rangle^i$	Intrinsic spatial average of c_i, (mol m^{-3}).
$\langle c\rangle$	Spatial average concentration (mol m^{-3}).
$\langle c\rangle^{\gamma\omega}$	Weighted spatial average concentration (mol m^{-3}).
$\tilde{c}_i$	Solute concentration standard deviation in the i-phase, (mol m^{-3}).
$\hat{c}_i$	Solute concentration peculiar deviation in the i-phase, (mol m^{-3}).
$\mathcal{D}a$	Microscopic Damköhler number, (−).
$\mathbf{D}_i$	Diffusion tensor in the i-phase, (m^2 s^{-1}).
$\mathbf{D}^*$	Dispersion tensor of the one-equation non-equilibrium model, (m^2 s^{-1}).
D^*_{xx}	xx-component of $\mathbf{D}^*$, (m^2 s^{-1}).
$\mathbf{D}^*_{Equ}$	Dispersion tensor of the one-equation local mass equilibrium model, (m^2 s^{-1}).
D^*_{xxEqu}	xx-component of $\mathbf{D}_{Equ}$, (m^2 s^{-1}).
D_Σ	Diffusion ratio between the ω-phase and the γ-phase, (−).
$\mathbf{D}^{**}_{ij}$	Dispersion tensors of the two-equation model, (m^2 s^{-1}).
h	Mass exchange coefficient of the two-equation model, (s^{-1}).
$\mathcal{K}$	Substrate half-saturation concentration, (mol m^{-3}).
k	Specific substrate half-saturation concentration, (mol kg^{-1} s^{-1}).
L	Characteristic length of the field-scale, (m).
l_i	Characteristic length of i-phase, (m).
l_k	The three lattice vectors that are needed to describe the 3-D spatial periodicity, (m).
L_c	Length of the representative cell, (m).
$\mathbf{n}_{ij}$	Normal vector poiting from the i-phase toward the j-phase, (−).
$\mathcal{P}e$	Microscopic Péclet number, (−).
R_0	Radius of the REV, (m).
$\mathcal{R}_\omega$	Reaction in the ω-phase, (mol m^{-3} s^{-1}).
$\mathcal{S}_{ij}$	Euclidean space defining the boundary between the i-phase and the j-phase, (−).
S_{ij}	Lebesgue measure of S_{ij} (area of the interface), (m^2).
s_i	Closure parameter in the i-phase associated to $\langle c\rangle^{\gamma\omega}$, (−).
t	Time, (s).
t'	Dimensionless time, (−).
$\mathbf{v}_i$	Velocity at the microscopic scale in the i-phase, (m s^{-1}).
$\mathbf{v}_i'$	Normalized velocity at the microscopic scale in the i-phase, (−).
$\langle\mathbf{v}_i\rangle$	Superficial spatial average of $\mathbf{v}_i$, (m s^{-1}).
$\langle\mathbf{v}_i\rangle^i$	Intrinsic spatial average of $\mathbf{v}_i$, (m s^{-1}).
$\langle v_i\rangle^i$	Norm of the intrinsic spatial average of $\mathbf{v}_i$, (m s^{-1}).
$\tilde{\mathbf{v}}_i$	Velocity standard deviation in the i-phase, (m s^{-1}).
$\mathbf{v}^*$	Effective velocity of the one-equation non-equilibrium model, (m s^{-1}).
v^*_x	x-component of $\mathbf{v}^*$, (m s^{-1}).
$\mathbf{v}^*_{Equ}$	Effective velocity of the one-equation local mass equilibrium model, (m s^{-1}).
$\mathcal{V}_i$	Euclidean space defining the i-phase, (−).
V_i	Lebesgue measure of $\mathcal{V}_i$ (volume of the i-phase), (m^3).
$\mathcal{V}$	Euclidean space defining the REV, (−).
V	Lebesgue measure of $\mathcal{V}$ (volume of the REV), (m^3).
$\mathbf{V}^{**}_{ij}$	Velocities of the two-equation model, (m s^{-1}).
$\mathbf{w}$	Velocity of the fluid–biofilm interface, (m s^{-1}).

Greek symbols

α	Substrate uptake rate parameter, (mol m^{-3} s^{-1}).
α^*	Effective reaction rate of the one-equation non-equilibrium model, (s^{-1}).
α^*_{Equ}	Effective reaction rate of the one-equation local mass equilibrium model, (s^{-1}).
γ-phase	Water-phase, (−).
ε_i	i-phase volumic fraction, (−).
ω-phase	Biofilm-phase, (−).
$\langle\rho_b\rangle$	Microbial concentration, (kg m^{-3}).
σ-phase	Grain-phase, (−).

Subscripts, superscripts

i,j	Indexes for γ or ω, (−).
k	Index for x, y or z (Cartesian coordinate system), (−).

separated by several orders of magnitude. This Monod expression can be extended to include both electron acceptor and electron donor concentrations.

If one started using Eq. (1) as an empirical representation of the mass transport and reaction process, it would not be immediately obvious how the microscale processes influence each of the macroscale

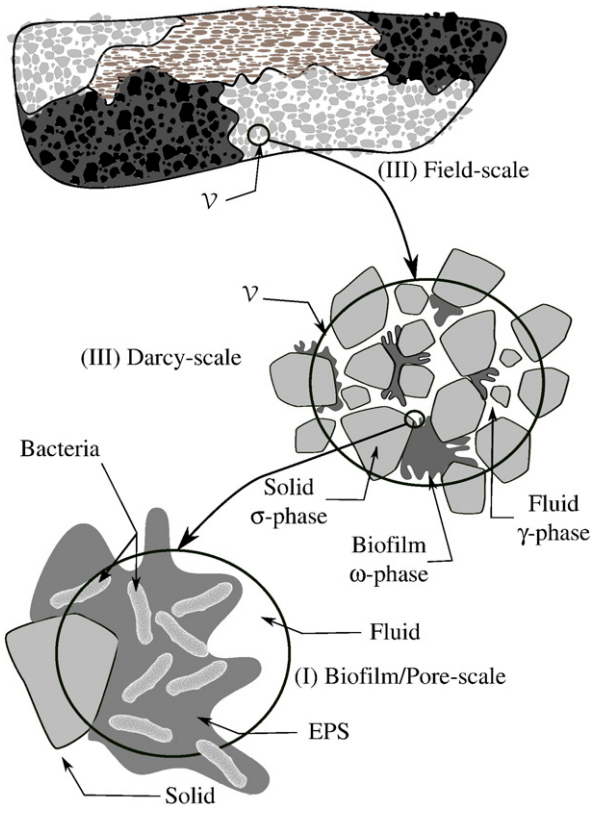

Fig. 1. Hierarchy of the main scales.

parameters that appear in the balance. To understand how information is passed through the scales of observation, it is necessary to start by considering the microscale physics of the phenomena. At the pore-scale, biofilms in porous media are usually represented by convective–diffusive processes within the fluid γ-phase, and diffusive-reactive processes within the biofilm ω-phase. This representation is built on three assumptions: 1) the biofilm is thick enough to be treated as a continuum [17,19], 2) the rate of reaction of planktonic cells (suspended in the water-phase) can be neglected compared to biofilms species (fixed on a surface and embedded within extracellular polymeric substances), and 3) the microscale channels that sometimes form within the biofilms are treated as part of the continuous fluid-phase. The mass exchange process between the fluid and biofilm phases is described by a continuity of the flux and of the concentrations at the interface, and a zero-flux condition is applied to the solid boundaries. Eq. (1) represents a one-equation approximation of all these processes at the Darcy-scale. Such an approach is frequently used in the literature, although merely one physical situation, referred to as the local mass equilibrium assumption, has been clearly identified to be properly described by only $\langle c_\gamma \rangle^\gamma$. In this case, the averaged concentrations in both phases are considered equal (strictly speaking, linked by a thermodynamical constant often close to unity) at any given time. In other words, when the gradients of the pointwise concentrations within each phase can be neglected, the continuity at the interface between the biofilms and the water-phases can be extended to the bulk phases and the modelization can be undertaken using a one-equation model Eq. (1).

1.2. Two-equation models

Along with the identification of these limitations, models that capture more physics of the reactive transport have been developed. The fluid–biofilm system has some obvious similarities to mobile–immobile (two-region, two equation) models, and one might consider a two-region model for biofilms in porous media under some circumstances. Several models have been devised with an explicit representation of the multiple-region aspects of the reactive transport. These include the *microcolony* [20] and *idealized biofilm* [21–24] models in which the porous medium is decomposed into a solid impermeable grain, a diffusive-reactive biofilm, a diffusive boundary layer and an advective–diffusive bulk water-phase. This representation leads to two-equation models where each equation describes the behavior of the averaged concentration on one single phase, and there is exchange between phases sharing common boundaries. Such models are able to capture more complex dynamics than one-equation local mass equilibrium models. Unfortunately, there are still two difficulties with such representations.

Problem 1. There is only an intuitive (rather than formal) relationship between the problem at the microscale and the one at the Darcy-scale. Hence, (1) it is still unclear when this model should be applied instead of the one-equation local mass equilibrium model for example, and (2) the dependence of the effective parameters (dispersion, effective velocities, mass exchange coefficients and effective reaction rate) on the microscale processes and geometry remains unknown.

Problem 2. The system of differential equations that need to be solved is more complex, and, thus, is more difficult to use in applications.

As a solution to the *Problem 1*, one can find a more precise connection between the macroscopic model and the associated microscale boundary value problem through upscaling methods. The physics of non-reactive transport has been widely addressed by deterministic techniques such as homogenization, moments matching and volume averaging with closure. Such approaches have been adapted to the problem of reactive transport with biofilms in porous media. These include the work of Wood et al. [25] and Golfier et al. [26] who used the volume averaging with closure theory [27] to compute effective parameters of the medium. However, except for two limit cases that have been studied by Orgogozo et al. [28], most of the work with volume averaging has focused on the local mass equilibrium assumption which is often excessively restrictive. To address the non-equilibrium situation in this two-phase configuration, one could consider two-equation models Eqs. (2a) and (2b)

$$\varepsilon_\gamma \frac{\partial \langle c_\gamma \rangle^\gamma}{\partial t} + \mathbf{V}^{**}_{\gamma\gamma} \cdot \nabla \langle c_\gamma \rangle^\gamma + \mathbf{V}^{**}_{\gamma\omega} \cdot \nabla \langle c_\omega \rangle^\omega = \nabla \cdot \left(\mathbf{D}^{**}_{\gamma\gamma} \cdot \nabla \langle c_\gamma \rangle^\gamma \right) + \nabla \cdot \left(\mathbf{D}^{**}_{\gamma\omega} \cdot \nabla \langle c_\omega \rangle^\omega \right) - h^{**} \left(\langle c_\gamma \rangle^\gamma - \langle c_\omega \rangle^\omega \right) \tag{2a}$$

$$\varepsilon_\omega \frac{\partial \langle c_\omega \rangle^\omega}{\partial t} + \mathbf{V}^{**}_{\omega\gamma} \cdot \nabla \langle c_\gamma \rangle^\gamma + \mathbf{V}^{**}_{\omega\omega} \cdot \nabla \langle c_\omega \rangle^\omega = \nabla \cdot \left(\mathbf{D}^{**}_{\omega\gamma} \cdot \nabla \langle c_\gamma \rangle^\gamma \right) + \nabla \cdot \left(\mathbf{D}^{**}_{\omega\omega} \cdot \nabla \langle c_\omega \rangle^\omega \right) - h^{**} \left(\langle c_\omega \rangle^\omega - \langle c_\gamma \rangle^\gamma \right) + \mathcal{R}_\omega. \tag{2b}$$

Here, $\langle c_i \rangle^i$ is the concentration of the solute in the i-phase. $\mathbf{V}^{**}_{ij}$ and $\mathbf{D}^{**}_{ij}$ (i and j are dummy indexes for γ, water-phase, or ω, biofilm-phase) are the macroscopic velocities and dispersion tensors of the two-equation model and h^{**} is the mass exchange coefficient. Eqs. (2a) and (2b) can be seen as a general compact way to write dual continua models [29–35]. The previous denominations refer to the scale of application and the physical processes involved whereas the two-equation model definition refers to the mathematical structure of the problem. These have been extensively used in hydrology and chemical engineering to describe the non-reactive mass transport in matrix-fracture media [36], in two-region large-scale systems [37] as well as for the heat transfer [38] in two-phase/region porous media. However, the complexity of the problem is still quite intimidating and the dilemma of reconciling Problem 1 and Problem 2 in a non-equilibrium situation appears fundamental.

1.3. A one-equation non-equilibrium model

There has been some interesting work suggesting that it is possible to develop a one-equation model that applies to non-equilibrium conditions under some time-constraints. Cunningham and Mendoza-Sanchez in [21] compared the behaviors of the one-equation model Eq. (1) ("the simple model") and the "idealized biofilm" model. They show that these are equivalent under steady state conditions and "effectively indistinguishable when the rate-controlling process is either external mass transfer or internal mass transfer" under transient conditions. From a more fundamental perspective, Zanotti and Carbonell showed in [39] that, for the non-reactive case, two-equation models have a time-asymptotic behavior which can be described in terms of a one-equation model. The demonstration is based on the moments matching principle at long times and does not assume local mass equilibrium. They considered the time-infinite behavior of the first two centered moments of a two-equation model developed using the volume averaging with closure theory. The essential idea here is that the time-asymptotic behavior of a multidomain formulation can be undertaken using a one-equation model even in a non-equilibrium (i.e., where the concentrations in the two regions are not at equilibrium relative to one another at any given time) situation.

One could follow the approach of Zanotti and Carbonell to develop an upscaled theory for the reactive case, but their approach is not straightforward. For example, in the reactive case it is not possible to adopt a time-infinite limit of the zeroth order moment. This is primarily because the chemical species is consumed by the micro-organisms and, consequently, its mass tends toward zero. One resolution is to consider only the smallest eigenvalue of the spatial operator for capturing the long-time rate of consumption. However, this approach leads to a very complex two-step analysis.

Upscaling the one-equation time-asymptotic model in one-step would be a useful development. Dykaar and Kitanidis devised such a technique in [40] starting directly from the microscale boundary value problem and using a Taylor–Aris–Brenner moment analysis. In their approach, they computed the dispersion tensor, the effective reaction rate and the effective solute velocity of a model porous medium with biofilm. However, there are two areas in this previous work that could be improved; these are as follows:

1. They considered a macroscopic average of the solute concentration only on the fluid-phase and, while the model does not assume local mass equilibrium, it is ambiguous as to what the specific model limitations are.
2. The moments matching technique in their analysis [40] makes the assumption that the behavior of the third and higher spatial moments can be neglected and that only the smallest eigenvalue of the spatial operator can be considered to describe the reaction rate. These hypotheses have different meanings in the single phase configuration and in the multiphase situation. In the work by Dykaar and Kitanidis, it is not clear how the phase configuration applies to the analysis.

In the non-reactive case, it has been proven [41] that the two-step method proposed by Zanotti and Carbonell is strictly equivalent to a one-step technique based on a particular volume averaging theory presented in that work. The essential feature of that theory is the definition of a useful, but unusual, perturbation decomposition. This decomposition is usually undertaken using fluctuations, conventionally defined in applications to subsurface hydrology by Gray [42]. For that kind of description, the pointwise concentration is expressed as an intrinsic averaged on the phase plus a perturbation. In an n-phase system, this decomposition leads to an n-equation macroscopic system and in our case would lead to the two-equation model previously discussed. Rather than using an intrinsic averaged on each phase, the perturbation concept can be extended to a weighted volume averaging $\langle c\rangle^{\gamma\omega}$ of the pointwise concentration on all the different phases Eq. (3), leading to a one-equation model. It is defined as

$$\langle c\rangle^{\gamma\omega} = \frac{\varepsilon_\gamma}{\varepsilon_\gamma+\varepsilon_\omega}\left\langle c_\gamma\right\rangle^{\gamma} + \frac{\varepsilon_\omega}{\varepsilon_\gamma+\varepsilon_\omega}\langle c_\omega\rangle^{\omega} \tag{3}$$

where ε_i is the volumic fraction occupied by the i-phase.

In this study, we use this variant of the technique of volume averaging with closure in the reactive case to develop a one-equation model. This model is different from those based on the local mass equilibrium assumption in that it does not impose specific conditions regarding the concentration in the two phases at any given time. Rather, it requires only that at long times the resulting balance equation is fully described by an advection–dispersion–reaction type equation, that is, by its first two spatial moments. This assumption means that the transport process is dispersive, and that the reactions do not themselves lead to spatial asymmetries for an initially symmetric solute distribution. This is very much in the spirit of the work by Dykaar and Kitanidis except that our model Eq. (4) describes the total mass present in the system and, hence, exhibits different effective velocity $\mathbf{v}^*$, dispersion tensor $\mathbf{D}^*$ and reaction rate α^*. The constraints associated with the theoretical development are extensively discussed.

$$\frac{\partial\langle c\rangle^{\gamma\omega}}{\partial t} + \mathbf{v}^*\cdot\nabla\langle c\rangle^{\gamma\omega} = \nabla\cdot\left(\mathbf{D}^*\cdot\nabla\langle c\rangle^{\gamma\omega}\right) - \alpha^*\langle c\rangle^{\gamma\omega}. \tag{4}$$

The remainder of the article is organized as follows. First, we derive the one-equation non-equilibrium reactive model. The microscopic equations describing the system at the pore-scale are written and we use the volume averaging upscaling process; we define a unique fluctuation that is subsequently used to obtain a macroscopic (but unclosed) one-equation model. Then, we establish a link between the two scales through closure problems. Finally, we show that a closed form of the macroscopic equation can be obtained where effective parameters depend explicitly upon closure variables solved over a representative cell. We explore numerically some solutions to the closure problem, and compare the non-equilibrium model to (1) the local equilibrium model and (2) pore-scale simulations.

2. Microscopic equations

Our study starts with the pore-scale description of the transport of a contaminant/nutrient in the porous medium. In the fluid (γ) phase, convective and diffusive transport are considered, and it is assumed that there is no reaction. In the biofilm (ω) phase, only diffusive transport and a reaction are considered. For the purposes of this paper, the velocity field is assumed to be known pointwise as a vector field. Mass balanced equations for the biofilm–fluid–solid system take the following form

$$\gamma\text{–}phase: \quad \frac{\partial c_\gamma}{\partial t} + \nabla\cdot\left(c_\gamma\mathbf{v}_\gamma\right) = \nabla\cdot\left(\mathbf{D}_\gamma\cdot\nabla c_\gamma\right) \tag{5}$$

$$BC1: \quad -\left(\mathbf{n}_{\gamma\sigma}\cdot\mathbf{D}_\gamma\right)\cdot\nabla c_\gamma = 0 \qquad \text{on } \mathcal{S}_{\gamma\sigma} \tag{6a}$$

$$BC2: \quad c_\omega = c_\gamma \qquad \text{on } \mathcal{S}_{\gamma\omega} \tag{6b}$$

$$BC3: \quad -\left(\mathbf{n}_{\gamma\omega}\cdot\mathbf{D}_\gamma\right)\cdot\nabla c_\gamma = -\left(\mathbf{n}_{\gamma\omega}\cdot\mathbf{D}_\omega\right)\cdot\nabla c_\omega \quad \text{on } \mathcal{S}_{\gamma\omega} \tag{6c}$$

$$BC4: \quad -(\mathbf{n}_{\omega\sigma}\cdot\mathbf{D}_\omega)\cdot\nabla c_\omega = 0 \qquad \text{on } \mathcal{S}_{\omega\sigma} \tag{6d}$$

$$\omega\text{–}phase: \frac{\partial c_\omega}{\partial t} = \nabla\cdot(\mathbf{D}_\omega\cdot\nabla c_\omega) + \mathcal{R}_\omega. \tag{7}$$

Here, c_γ is the chemical species concentration in the γ-phase, and c_ω is the concentration in the ω-phase (which can be interpreted as the volume average concentration in the extracellular space [19,25]). The symbols $\mathbf{D}_\gamma$ and $\mathbf{D}_\omega$ represent the diffusion tensors in the γ and ω-phases, respectively; $\mathcal{R}_\omega$ is the reaction rate in the ω-phase, the formulation of this term is detailed in Section 3.5; $\mathbf{n}_{\gamma\omega}$ is the unit normal pointing from the γ-phase to the ω-phase; $\mathbf{n}_{\gamma\sigma}$ is the unit normal pointing from the γ-phase to the σ-phase; $\mathbf{n}_{\omega\sigma}$ is the unit normal pointing from the ω-phase to the σ-phase; $\mathcal{S}_{\gamma\omega}$ is the Euclidean space representing the interface between the γ-phase and the ω-phase; $\mathcal{S}_{\gamma\sigma}$ is the interface between the γ-phase and the σ-phase; and $\mathcal{S}_{\omega\sigma}$ is the interface between the ω-phase and the ω-phase.

3. Upscaling

3.1. Average definitions

To obtain a macroscopic equation for the mass transport at the Darcy-scale, we average each microscopic equation at the pore-scale over a representative region (REV), $\mathcal{V}$ Figs. 1 and 2. $\mathcal{V}_\gamma$ and $\mathcal{V}_\omega$ are the Euclidean spaces representing the γ- and ω-phases in the REV. V_γ and V_ω are the Lebesgue measures of $\mathcal{V}_\gamma$ and $\mathcal{V}_\omega$, that is, the volumes of the respective phases. The Darcy-scale *superficial* average of c_i (where i represents γ or ω) is defined the following way

$$\left\langle c_\gamma\right\rangle = \frac{1}{V}\int_{\mathcal{V}_\gamma(\mathbf{x},t)} c_\gamma dV, \langle c_\omega\rangle = \frac{1}{V}\int_{\mathcal{V}_\omega(\mathbf{x},t)} c_\omega dV. \tag{8}$$

Then, we define *intrinsic* averaged quantities

$$\left\langle c_\gamma\right\rangle^{\gamma} = \frac{1}{V_\gamma(\mathbf{x},t)}\int_{\mathcal{V}_\gamma(\mathbf{x},t)} c_\gamma dV, \langle c_\omega\rangle^{\omega} = \frac{1}{V_\omega(\mathbf{x},t)}\int_{\mathcal{V}_\omega(\mathbf{x},t)} c_\omega dV. \tag{9}$$

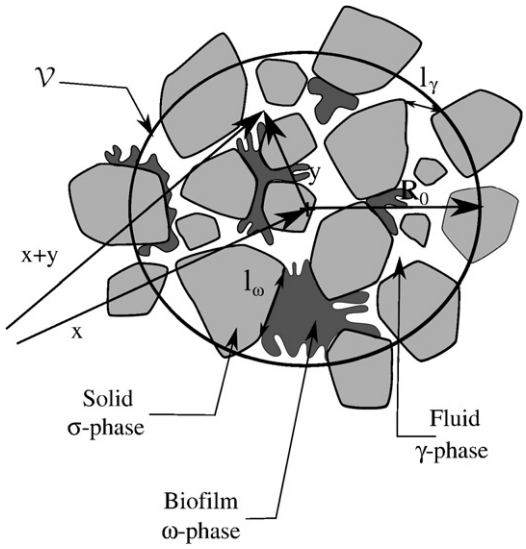

Fig. 2. Pore-scale description of a Darcy-scale averaging volume.

Volumes $V_\gamma(\mathbf{x},t)$ and $V_\omega(\mathbf{x},t)$ are related to the volume V by

$$\varepsilon_\gamma(\mathbf{x},t)=\frac{V_\gamma(\mathbf{x},t)}{V},\varepsilon_\omega(\mathbf{x},t)=\frac{V_\omega(\mathbf{x},t)}{V}. \tag{10}$$

Hence, we have

$$\left\langle c_\gamma\right\rangle=\varepsilon_\gamma(\mathbf{x},t)\left\langle c_\gamma\right\rangle^\gamma,\langle c_\omega\rangle=\varepsilon_\omega(\mathbf{x},t)\langle c_\omega\rangle^\omega. \tag{11}$$

Due to the growth process, the geometry associated with the biofilm-phase can evolve in time. However, we will assume that changes in the V_γ and V_ω volumes are decoupled from the transport problem. There is substantial support for this approximation because the characteristic time for growth is much larger than the characteristic time for transport processes [17,18]. Moreover, volumic fractions ε_γ and ε_ω are also supposed constant in space so that we consider a homogeneous porous medium.

As stated above, the goal of this article is to devise a one-equation model that describes the evolution of the solute mass in the two phases by a single equation at the Darcy-scale. Toward that end, we define two additional macroscopic concentrations. The first is the spatial average concentration, defined by

$$\langle c\rangle=\varepsilon_\gamma\left\langle c_\gamma\right\rangle^\gamma+\varepsilon_\omega\langle c_\omega\rangle^\omega. \tag{12}$$

The second is a volume-fraction weighted averaged concentration [17,43]

$$\langle c\rangle^{\gamma\omega}=\frac{\varepsilon_\gamma}{\varepsilon_\gamma+\varepsilon_\omega}\left\langle c_\gamma\right\rangle^\gamma+\frac{\varepsilon_\omega}{\varepsilon_\gamma+\varepsilon_\omega}\langle c_\omega\rangle^\omega. \tag{13}$$

During the averaging process, there arise terms involving the point values for c_γ, c_ω, and $\mathbf{v}_\gamma$. To treat these terms conventionally, one defines perturbation decompositions as follows

$$c_\gamma=\left\langle c_\gamma\right\rangle^\gamma+\tilde{c}_\gamma \tag{14}$$

$$c_\omega=\langle c_\omega\rangle^\omega+\tilde{c}_\omega \tag{15}$$

$$\mathbf{v}_\gamma=\left\langle \mathbf{v}_\gamma\right\rangle^\gamma+\tilde{\mathbf{v}}_\gamma. \tag{16}$$

With these decompositions, the averaging process would lead to the formulation of a two-equation model, where a separate upscaled equation would be developed for each phase.

We will adopt a fundamentally different concentration decomposition which allows the development of a one-equation model that is different from the one-equation model that assumes local mass equilibrium. To do so, we define the weighted averaged concentration, $\langle c\rangle^{\gamma\omega}$ by the decompositions

$$c_\gamma=\langle c\rangle^{\gamma\omega}+\hat{c}_\gamma \tag{17a}$$

$$c_\omega=\langle c\rangle^{\gamma\omega}+\hat{c}_\omega. \tag{17b}$$

Notice that with this definition, we do not generally have the condition that the intrinsic average of the deviation is zero, i.e., $\langle\tilde{c}_\gamma\rangle^\gamma,\langle\tilde{c}_\omega\rangle^\omega=0$. However, we do have a generalization of this idea in the form

$$\varepsilon_\omega\langle\hat{c}_\omega\rangle^\omega+\varepsilon_\gamma\left\langle\hat{c}_\gamma\right\rangle^\gamma=0. \tag{18}$$

3.2. Averaging equations

To start, the averaging operators and decompositions defined above are applied to Eqs. (5) and (7); the details of this process are provided in Appendix A. The result is

γ−phase

$$\begin{aligned}&\frac{\partial\varepsilon_\gamma\left\langle c_\gamma\right\rangle^\gamma}{\partial t}+\nabla\cdot\left(\varepsilon_\gamma\left\langle c_\gamma\right\rangle^\gamma\left\langle\mathbf{v}_\gamma\right\rangle^\gamma\right)\\&\quad=\nabla\cdot\left\{\varepsilon_\gamma\mathbf{D}_\gamma\cdot\ \nabla\left\langle c_\gamma\right\rangle^\gamma+\frac{1}{\mathcal{V}_\gamma}\int_{\mathcal{S}_{\gamma\omega}}\mathbf{n}_{\gamma\omega}\tilde{c}_\gamma dS+\frac{1}{\mathcal{V}_\gamma}\int_{\mathcal{S}_{\gamma\sigma}}\mathbf{n}_{\gamma\sigma}\tilde{c}_\gamma dS\right)\Bigg\}\\&\qquad+\frac{1}{\mathcal{V}}\int_{\mathcal{S}_{\gamma\omega}}(\mathbf{n}_{\gamma\omega}\cdot\mathbf{D}_\gamma)\cdot\nabla c_\gamma dS+\frac{1}{\mathcal{V}}\int_{\mathcal{S}_{\gamma\sigma}}(\mathbf{n}_{\gamma\sigma}\cdot\mathbf{D}_\gamma)\cdot\nabla c_\gamma dS-\nabla\cdot\left\langle\tilde{c}_\gamma\tilde{\mathbf{v}}_\gamma\right\rangle\end{aligned} \tag{19}$$

ω−phase

$$\begin{aligned}\frac{\partial\varepsilon_\omega\langle c_\omega\rangle^\omega}{\partial t}&=\nabla\cdot\left\{\varepsilon_\omega\mathbf{D}_\omega\cdot\left(\nabla\langle c_\omega\rangle^\omega+\frac{1}{\mathcal{V}_\omega}\int_{\mathcal{S}_{\omega\gamma}}\mathbf{n}_{\omega\gamma}\tilde{c}_\omega dS+\frac{1}{\mathcal{V}_\omega}\int_{\mathcal{S}_{\omega\sigma}}\mathbf{n}_{\omega\sigma}\tilde{c}_\omega dS\right)\right\}\\&\quad+\frac{1}{\mathcal{V}}\int_{\mathcal{S}_{\omega\gamma}}(\mathbf{n}_{\omega\gamma}\cdot\mathbf{D}_\omega)\cdot\nabla c_\omega dS+\frac{1}{\mathcal{V}}\int_{\mathcal{S}_{\omega\sigma}}(\mathbf{n}_{\omega\sigma}\cdot\mathbf{D}_\omega)\cdot\nabla c_\omega dS+\varepsilon_\omega\langle\mathcal{R}_\omega\rangle^\omega\end{aligned} \tag{20}$$

3.3. The macroscopic concentration in a multiphase system

At this point, it is clear that in general one needs two macroscale equations to describe the system (one-equation for each phase). It is not obvious, however, if there are conditions for which the mass transport can be represented using a single concentration and what should be the definition of this macroscopic measure in a multiphase configuration. For example, experimentally, biofilms are often studied in laboratory devices such as columns. One may then ask the questions (1) "What concentration are we measuring at the output of a column colonized by biofilm?" and (2) "How do we establish a relationship between this experimental measure and the concentration in our model?"

We begin by addressing the first question. The concentration measured in an experimental system depends on the design of the experimental system, the physical and chemical properties of the porous medium, and on the experimental device used to make measurements. As an example, assume that we are trying to obtain the elution curve of a tracer (concentration c_i in the i-phase) at the output of the column by sampling the water on relatively small time intervals ΔT (say, a hundred samples for one elution curve) and then measuring the concentration within each volume. For high microscopic Péclet numbers, one may measure a quantity close to $\langle c_\gamma\rangle^\gamma$ as the

transport is driven by the convection in the water-phase. For microscopic Péclet numbers lower than unity, that is, a transport driven by diffusion, one may measure something closer to $\langle c\rangle^{\gamma\omega}$. In this context, a general definition of the concentration would be

$$\langle C\rangle = \int_0^t \int_{\mathcal{V}} G(\mathbf{x}-\mathbf{y}, t-\tau) c(\mathbf{y},\tau) dV(\mathbf{y}) d\tau \tag{21}$$

where G is a spatio-temporal kernel corresponding to a weighting function accounting for the measurement device, the column device and the physics of the transport, and c is the concentration defined by

$$c = \left\{ \begin{array}{l} c_\gamma \text{ in the } \gamma-\text{phase} \\ c_\omega \text{ in the } \omega-\text{phase} \\ 0 \text{ in the } \sigma-\text{phase} \end{array} \right\}. \tag{22}$$

Then, it is necessary to address question (2), that is, we must find a relationship between $\langle C\rangle$ and the concentrations appearing in our models. There are two different ways to proceed. First, it is possible to formulate a generalized volume averaging theory to directly describe the transport of $\langle C\rangle$. This has been proposed in [44]. Second, it is feasible to describe the transport of a relatively simple averaged concentration and to apply the correct kernel *a posteriori*. In this case, the concentration to be used in the model can be chosen on the basis of its relevance from a theoretical point of view.

In this article, we use $\langle c\rangle^{\gamma\omega}$ [Eq. (17a)] as a macroscopic concentration, that is, we are interested in following the spatio-temporal macroscopic evolution of the total component mass in the porous medium. One significant advantage of this definition is that, in a non-reactive medium, the concentration $\langle c\rangle^{\gamma\omega}$ is conservative; unlike the individual phase averages, which are not conservative due to interphase mass transfer. For example, $\langle c_\gamma\rangle^{\gamma}$ is often used as a macroscopic concentration but looses many features of the transport processes. Then, to go back to $\langle C\rangle$, one needs to determine the kernel F defined by

$$\langle C\rangle = \int_0^t \int_{\mathcal{V}} F(\mathbf{x}-\mathbf{y}, t-\tau) \langle c\rangle^{\gamma\omega}(\mathbf{y},\tau) dV(\mathbf{y}) d\tau. \tag{23}$$

The precise determination of the kernel G or F represents an extremely difficult task; in real problems, one can usually only approximate the correct concentration to use for a specific problem because the kernel functions are generally not exactly known.

3.4. Development of the macroscopic balance equation

In order to obtain a single equation for describing the balance of the concentration $\langle c\rangle^{\gamma\omega}$, we need to combine the two macroscopic equations given by Eqs. (19) and (20). It is then necessary to eliminate all intrinsic concentrations, $\langle c_i\rangle^{i}$, by combining terms. This kind of description can be developed using the nonconventional decompositions defined by $\langle c\rangle^{\gamma\omega}$ [45] which naturally arises when summing Eqs. (19) and (20). We have applied this kind of analysis to the two macroscale equations developed above; the detailed derivation can be found in Appendix B. The following non-closed equation results from that analysis

$$\begin{aligned} &\frac{\partial \langle c\rangle^{\gamma\omega}}{\partial t} + \nabla\cdot\left(\frac{\varepsilon_\gamma}{\varepsilon_\gamma+\varepsilon_\omega} \langle c\rangle^{\gamma\omega} \left\langle \mathbf{v}_\gamma \right\rangle^{\gamma} \right) \\ &= \nabla\cdot\left\{ \left(\frac{\varepsilon_\omega}{\varepsilon_\gamma+\varepsilon_\omega}\mathbf{D}_\omega + \frac{\varepsilon_\gamma}{\varepsilon_\gamma+\varepsilon_\omega}\mathbf{D}_\gamma \right)\cdot\nabla\langle c\rangle^{\gamma\omega} \right\} - \frac{1}{\varepsilon_\gamma+\varepsilon_\omega}\nabla\cdot\left\langle \hat{c}_\gamma \mathbf{v}_\gamma \right\rangle \\ &\quad + \nabla\cdot\left(\frac{\varepsilon_\omega}{\varepsilon_\gamma+\varepsilon_\omega}\mathbf{D}_\omega\cdot\left\langle \nabla\hat{c}_\omega \right\rangle^{\omega} + \frac{\varepsilon_\gamma}{\varepsilon_\gamma+\varepsilon_\omega}\mathbf{D}_\gamma\cdot\left\langle \nabla\hat{c}_\gamma \right\rangle^{\gamma} \right) \\ &\quad + \frac{\varepsilon_\omega}{\varepsilon_\gamma+\varepsilon_\omega}\langle \mathcal{R}_\omega\rangle^{\omega}. \end{aligned} \tag{24}$$

3.5. Reaction term

The form of the reaction rate has not yet been detailed but, at this point, it is important to make further progress concerning this aspect of the problem. The classical dual-Monod [46] reaction rate for electron donor A and acceptor B, is widely adopted to describe biofilm substrate uptake and growth in systems with a single substrate and a single terminal electron acceptor. In this case, the reaction rate is given by a hyperbolic kinetic expression of the form

$$\mathcal{R}_\omega = -\alpha \frac{c_{A\omega}}{c_{A\omega}+\mathcal{K}_A} \frac{c_{B\omega}}{c_{B\omega}+\mathcal{K}_B}. \tag{25}$$

Here, the α is the substrate uptake rate parameter (often expanded as $\alpha = k\langle\rho_b\rangle$, where k is the specific substrate uptake rate parameter, and $\langle\rho_b\rangle$ is the microbial concentration; cf. [47]). One often considers the case where the electron is not limiting $c_{B\omega} \gg \mathcal{K}_B$, in which case the kinetics take the classical Monod form

$$\mathcal{R}_\omega = -\alpha \frac{c_{A\omega}}{c_{A\omega}+\mathcal{K}_A} \tag{26}$$

which can be written

$$\mathcal{R}_\omega = -\alpha \frac{c_\omega}{c_\omega+\mathcal{K}}. \tag{27}$$

This is beyond the scope of this paper to propose a technique to upscale such non-linear kinetics and we will only consider the linear case Eq. (28)

$$\mathcal{R}_\omega = -\frac{\alpha}{\mathcal{K}} c_\omega. \tag{28}$$

These linear kinetics can be seen as a particular case of the classical Monod for which $c_\omega \ll \mathcal{K}$, that is, a highly reactive biofilm or relatively low concentrations. This approximation has been undertaken incalculable times [48–50] and is discussed in [21,40].

3.6. Non-closed macroscopic formulation

Introducing linear kinetics in Eq. (24) leads to

$$\begin{aligned} &\frac{\partial \langle c\rangle^{\gamma\omega}}{\partial t} + \nabla\cdot\left(\frac{\varepsilon_\gamma}{\varepsilon_\gamma+\varepsilon_\omega} \langle c\rangle^{\gamma\omega} \left\langle \mathbf{v}_\gamma \right\rangle^{\gamma} \right) \\ &= \nabla\cdot\left\{ \left(\frac{\varepsilon_\omega}{\varepsilon_\gamma+\varepsilon_\omega}\mathbf{D}_\omega + \frac{\varepsilon_\gamma}{\varepsilon_\gamma+\varepsilon_\omega}\mathbf{D}_\gamma \right)\cdot\nabla\langle c\rangle^{\gamma\omega} \right\} \\ &\quad + \nabla\cdot\left(\frac{\varepsilon_\omega}{\varepsilon_\gamma+\varepsilon_\omega}\mathbf{D}_\omega\cdot\left\langle \nabla\hat{c}_\omega \right\rangle^{\omega} + \frac{\varepsilon_\gamma}{\varepsilon_\gamma+\varepsilon_\omega}\mathbf{D}_\gamma\cdot\left\langle \nabla\hat{c}_\gamma \right\rangle^{\gamma} \right) \\ &\quad - \frac{\varepsilon_\omega}{\varepsilon_\gamma+\varepsilon_\omega}\frac{\alpha}{\mathcal{K}}\left(\langle c\rangle^{\gamma\omega} + \langle \hat{c}_\omega\rangle^{\omega} \right) - \frac{1}{\varepsilon_\gamma+\varepsilon_\omega}\nabla\cdot\left\langle \hat{c}_\gamma \tilde{\mathbf{v}}_\gamma \right\rangle \\ &\quad - \frac{1}{\varepsilon_\gamma+\varepsilon_\omega}\nabla\cdot\left(\left\langle \hat{c}_\gamma \right\rangle \left\langle \mathbf{v}_\gamma \right\rangle^{\gamma} \right). \end{aligned} \tag{29}$$

Although Eq. (36) represents a macroscale mass transport equation, it is not yet under a conventional form because deviation concentrations still remain. Eliminating these deviation concentrations, and hence uncoupling the physics at the microscale from the physics at the macroscale, is referred to as the closure problem.

4. Closure

4.1. Deviation equations

To close Eq. (29), we first need to develop balance equations for the concentration deviations, $\hat{c}_\gamma$ and $\hat{c}_\omega$. Going back to their definitions Eq. (17a) suggests that these equations can be obtained by subtracting the averaged equation Eq. (24) to the microscopic mass balanced Eqs. (5) and (7). To make further progress, it is also necessary to make some simplifications. We will assume that all the terms containing only second order derivatives of surface integrated or volume averaged quantities are negligible as compared to spatial derivatives of fluctuation quantities over the REV. Terms containing derivatives of averaged quantities are often referred to as non-local terms. This means that these cannot be calculated locally on a REV; rather, they act as source terms and, if they cannot be neglected, that is, if the hypothesis of separation of length scales is not valid, they impose a coupling between the microscale and the macroscale problems.

Eq. (5) minus Eq. (24)

$$\begin{aligned}\frac{\partial \hat{c}_\gamma}{\partial t} + \nabla\cdot\left(\mathbf{v}_\gamma \hat{c}_\gamma\right) = \nabla\cdot\left(\mathbf{D}_\gamma\cdot\nabla\hat{c}_\gamma\right) - \nabla\cdot\left(\tilde{\mathbf{v}}_\gamma\langle c\rangle^{\gamma\omega}\right) - \frac{\varepsilon_\omega}{\varepsilon_\omega+\varepsilon_\gamma}\nabla\cdot\left(\left\langle\mathbf{v}_\gamma\right\rangle^\gamma\langle c\rangle^{\gamma\omega}\right)\\ -\nabla\cdot\left(\frac{\varepsilon_\omega}{\varepsilon_\gamma+\varepsilon_\omega}\mathbf{D}_\omega\cdot\langle\nabla\hat{c}_\omega\rangle^\omega + \frac{\varepsilon_\gamma}{\varepsilon_\gamma+\varepsilon_\omega}\mathbf{D}_\gamma\cdot\left\langle\nabla\hat{c}_\gamma\right\rangle^\gamma\right)\\ + \frac{\alpha}{\mathcal{K}}\frac{\varepsilon_\omega}{\varepsilon_\omega+\varepsilon_\gamma}\left(\langle c\rangle^{\gamma\omega} + \langle\hat{c}_\omega\rangle^\omega\right) + \frac{1}{\varepsilon_\gamma+\varepsilon_\omega}\nabla\cdot\left\langle\hat{c}_\gamma\mathbf{v}_\gamma\right\rangle.\end{aligned} \tag{30}$$

Eq. (7) minus Eq. (24)

$$\begin{aligned}\frac{\partial \hat{c}_\omega}{\partial t} = \nabla\cdot\left(\mathbf{D}_\omega\cdot\nabla\hat{c}_\omega\right) + \frac{\varepsilon_\gamma}{\varepsilon_\gamma+\varepsilon_\omega}\nabla\cdot\left(\left\langle\mathbf{v}_\gamma\right\rangle^\gamma\langle c\rangle^{\gamma\omega}\right)\\ -\nabla\cdot\left(\frac{\varepsilon_\omega}{\varepsilon_\gamma+\varepsilon_\omega}\mathbf{D}_\omega\cdot\langle\nabla\hat{c}_\omega\rangle^\omega + \frac{\varepsilon_\gamma}{\varepsilon_\gamma+\varepsilon_\omega}\mathbf{D}_\gamma\cdot\left\langle\nabla\hat{c}_\gamma\right\rangle^\gamma\right)\\ -\frac{\alpha}{\mathcal{K}}\frac{\varepsilon_\gamma}{\varepsilon_\omega+\varepsilon_\gamma}\langle c\rangle^{\gamma\omega} + \frac{\alpha}{\mathcal{K}}\frac{\varepsilon_\omega}{\varepsilon_\omega+\varepsilon_\gamma}\langle\hat{c}_\omega\rangle^\omega - \frac{\alpha}{\mathcal{K}}\hat{c}_\omega\\ + \frac{1}{\varepsilon_\gamma+\varepsilon_\omega}\nabla\cdot\left\langle\hat{c}_\gamma\mathbf{v}_\gamma\right\rangle.\end{aligned} \tag{31}$$

We will impose the condition that we are interested in primarily the asymptotic behavior of the system; thus, we can adopt a quasi-steady hypothesis. In essence, this constraint indicates that there is a separation of time scales for the relaxation of $\hat{c}_\gamma$ and $\hat{c}_\omega$ as compared to the time scale for changes in the average concentration, $\langle c\rangle^{\gamma\omega}$. Such constraints can be put in the form

$$\begin{aligned}T_\gamma^* &\gg \frac{l_\gamma^2}{||\mathbf{D}_\gamma||}, \frac{l_\gamma}{\left\langle v_\gamma\right\rangle^\gamma}\\ T_\omega^* &\gg \frac{l_\omega^2}{||\mathbf{D}_\omega||}, \frac{\mathcal{K}}{\alpha}\end{aligned} \tag{32}$$

where T_γ^* (respectively T_ω^*) is a characteristic time associated to $\frac{\partial\hat{c}_\gamma}{\partial t}$ (respectively $\frac{\partial\hat{c}_\omega}{\partial t}$); $||.||$ is the tensorial norm given by

$$||\mathbf{T}|| = \frac{1}{2}\sqrt{\mathbf{T}:\mathbf{T}} = \frac{1}{2}\sqrt{T_{ij}T_{ji}}. \tag{33}$$

The vector norm is given by

$$\left\langle v_\gamma\right\rangle^\gamma = \left(\left\langle\mathbf{v}_\gamma\right\rangle^\gamma\cdot\left\langle\mathbf{v}_\gamma\right\rangle^\gamma\right)^{\frac{1}{2}}. \tag{34}$$

This hypothesis is the key to understanding the time-asymptotic behavior of the model developed herein. It has been shown in [41,45], in the non-reactive case, that this quasi-stationarity assumption is equivalent to time-asymptotic models derived through moments analysis [39] from two-equation models. In other words, the assumption of quasi-stationarity on the $\hat{c}$ perturbations is much more restrictive than the one on $\tilde{c}$ which leads to the two-equation model. One other way of seeing it is to express $\hat{c}$ as

$$\hat{c}_i = \langle\hat{c}_i\rangle^i + \tilde{c}_i \tag{35}$$

so that

$$\frac{\partial\hat{c}_i}{\partial t} = \frac{\partial\langle\hat{c}_i\rangle^i}{\partial t} + \frac{\partial\tilde{c}_i}{\partial t}. \tag{36}$$

Hence, imposing constraints on $\frac{\partial\hat{c}_i}{\partial t}$ results in constraints on $\frac{\partial\tilde{c}_i}{\partial t}$ but also on $\frac{\partial\langle\hat{c}_i\rangle^i}{\partial t}$; in opposition to constraints only on $\frac{\partial\tilde{c}_i}{\partial t}$ in the two-equation quasi-stationary models. With these approximations, the closure problems can be rewritten as follows

$$\begin{aligned}\nabla\cdot(\mathbf{v}_\gamma\hat{c}_\gamma) = \nabla\cdot\left(\mathbf{D}_\gamma\cdot\nabla\hat{c}_\gamma\right) - \nabla\cdot\left(\tilde{\mathbf{v}}_\gamma\langle c\rangle^{\gamma\omega}\right) - \frac{\varepsilon_\omega}{\varepsilon_\omega+\varepsilon_\gamma}\nabla\cdot\left(\left\langle\mathbf{v}_\gamma\right\rangle^\gamma\langle c\rangle^{\gamma\omega}\right)\\ + \frac{\alpha}{\mathcal{K}}\frac{\varepsilon_\omega}{\varepsilon_\omega+\varepsilon_\gamma}\left(\langle c\rangle^{\gamma\omega} + \langle\hat{c}_\omega\rangle^\omega\right)\\ -\nabla\cdot\left(\frac{\varepsilon_\omega}{\varepsilon_\gamma+\varepsilon_\omega}\mathbf{D}_\omega\cdot\langle\nabla\hat{c}_\omega\rangle^\omega + \frac{\varepsilon_\gamma}{\varepsilon_\gamma+\varepsilon_\omega}\mathbf{D}_\gamma\cdot\left\langle\nabla\hat{c}_\gamma\right\rangle^\gamma\right)\\ + \frac{\varepsilon_\gamma}{\varepsilon_\gamma+\varepsilon_\omega}\left(\nabla\cdot\left\langle\hat{c}_\gamma\tilde{\mathbf{v}}_\gamma\right\rangle^\gamma + \left\langle v_\gamma\right\rangle^\gamma\cdot\nabla\left\langle\hat{c}_\gamma\right\rangle^\gamma\right)\end{aligned} \tag{37}$$

$$BC1: \quad -\left(\mathbf{n}_{\gamma\sigma}\cdot\mathbf{D}_\gamma\right)\cdot\nabla\hat{c}_\gamma = \left(\mathbf{n}_{\gamma\sigma}\cdot\mathbf{D}_\gamma\right)\cdot\nabla\langle c\rangle^{\gamma\omega} \quad \text{on } \mathcal{S}_{\gamma\sigma} \tag{38a}$$

$$BC2: \quad \hat{c}_\omega = \hat{c}_\gamma \quad \text{on } \mathcal{S}_{\gamma\omega} \tag{38b}$$

$$\begin{aligned}BC3: \quad -\left(\mathbf{n}_{\gamma\omega}\cdot\mathbf{D}_\gamma\right)\cdot\nabla\hat{c}_\gamma = -\left(\mathbf{n}_{\gamma\omega}\cdot\mathbf{D}_\omega\right)\cdot\nabla\hat{c}_\omega\\ -\left\{\mathbf{n}_{\gamma\omega}\cdot\left(\mathbf{D}_\omega-\mathbf{D}_\gamma\right)\right\}\cdot\nabla\langle c\rangle^{\gamma\omega} \quad \text{on } \mathcal{S}_{\gamma\omega}\end{aligned} \tag{38c}$$

$$BC4: \quad -(\mathbf{n}_{\omega\sigma}\cdot\mathbf{D}_\omega)\cdot\nabla\hat{c}_\omega = (\mathbf{n}_{\omega\sigma}\cdot\mathbf{D}_\omega)\cdot\nabla\langle c\rangle^{\gamma\omega} \quad \text{on } \mathcal{S}_{\omega\sigma} \tag{38d}$$

$$\begin{aligned}0 = \nabla\cdot(\mathbf{D}_\omega\cdot\nabla\hat{c}_\omega) + \frac{\varepsilon_\gamma}{\varepsilon_\gamma+\varepsilon_\omega}\nabla\cdot\left(\left\langle\mathbf{v}_\gamma\right\rangle^\gamma\langle c\rangle^{\gamma\omega}\right) - \frac{\alpha}{\mathcal{K}}\frac{\varepsilon_\gamma}{\varepsilon_\omega+\varepsilon_\gamma}\langle c\rangle^{\gamma\omega}\\ + \frac{\alpha}{\mathcal{K}}\frac{\varepsilon_\gamma}{\varepsilon_\omega+\varepsilon_\gamma}\langle\hat{c}_\omega\rangle^\omega - \frac{\alpha}{\mathcal{K}}\hat{c}_\omega\\ -\nabla\cdot\left(\frac{\varepsilon_\omega}{\varepsilon_\gamma+\varepsilon_\omega}\mathbf{D}_\omega\cdot\langle\nabla\hat{c}_\omega\rangle^\omega + \frac{\varepsilon_\gamma}{\varepsilon_\gamma+\varepsilon_\omega}\mathbf{D}_\gamma\cdot\left\langle\nabla\hat{c}_\gamma\right\rangle^\gamma\right)\\ + \frac{\varepsilon_\gamma}{\varepsilon_\gamma+\varepsilon_\omega}\left(\nabla\cdot\left\langle\hat{c}_\gamma\tilde{\mathbf{v}}_\gamma\right\rangle^\gamma + \left\langle\mathbf{v}_\gamma\right\rangle^\gamma\cdot\nabla\left\langle\hat{c}_\gamma\right\rangle^\gamma\right).\end{aligned} \tag{39}$$

4.2. Representation of the closure solution

The mathematical structure of this problem indicates that there are a number of nonhomogeneous quantities involving $\langle c\rangle^{\gamma\omega}$ that act as forcing terms. Under the conditions that a *local* macroscopic equation is

desired, it can be shown (c.f., [51]) that the general solution to this problem takes the form

$$\hat{c}_\gamma = \mathbf{b}_\gamma \cdot \nabla \langle c \rangle^{\gamma\omega} - s_\gamma \langle c \rangle^{\gamma\omega} \tag{40}$$

$$\hat{c}_\omega = \mathbf{b}_\omega \cdot \nabla \langle c \rangle^{\gamma\omega} - s_\omega \langle c \rangle^{\gamma\omega}. \tag{41}$$

Here, the variables $\mathbf{b}_\gamma$, $\mathbf{b}_\omega$, s_γ, and s_ω can be interpreted as integrals of the associated Greens functions for the closure problem. This closure fails to capture any characteristic time associated to the exchange between both phases in opposition to the closure used for two-equation models which describes one characteristic time associated with the exchange. Only non-local theories or direct pore-scale simulations would be able to recover all the characteristic times involved in this process.

Upon substituting this general form into the closure problem, we can collect terms involving $\nabla \langle c \rangle^{\gamma\omega}$ and $\langle c \rangle^{\gamma\omega}$. The result is the following set of closure problems in which derivatives of averaged quantities are neglected

Problem I (s-problem)

$$\nabla \cdot \left(\mathbf{v}_\gamma s_\gamma \right) = \nabla \cdot \left(\mathbf{D}_\gamma \cdot \nabla s_\gamma \right) - \frac{\alpha}{\mathcal{K}} \frac{\varepsilon_\omega}{\varepsilon_\omega + \varepsilon_\gamma} - \frac{\alpha}{\mathcal{K}} \frac{\varepsilon_\gamma}{\varepsilon_\omega + \varepsilon_\gamma} \left\langle s_\gamma \right\rangle^\gamma \tag{42}$$

$$BC1: \quad -\left(\mathbf{n}_{\gamma\sigma} \cdot \mathbf{D}_\gamma \right) \cdot \nabla s_\gamma = 0 \qquad \text{on } \mathcal{S}_{\gamma\sigma} \tag{43a}$$

$$BC2: \quad s_\omega = s_\gamma \qquad \text{on } \mathcal{S}_{\gamma\omega} \tag{43b}$$

$$BC3: \quad -\left(\mathbf{n}_{\gamma\omega} \cdot \mathbf{D}_\gamma \right) \cdot \nabla s_\gamma = -\left(\mathbf{n}_{\gamma\omega} \cdot \mathbf{D}_\omega \right) \cdot \nabla s_\omega \qquad \text{on } \mathcal{S}_{\gamma\omega} \tag{43c}$$

$$BC4: \quad -(\mathbf{n}_{\omega\sigma} \cdot \mathbf{D}_\omega) \cdot \nabla s_\omega = 0 \qquad \text{on } \mathcal{S}_{\omega\sigma} \tag{43d}$$

$$0 = \nabla \cdot (\mathbf{D}_\omega \cdot \nabla s_\omega) + \frac{\alpha}{\mathcal{K}} \frac{\varepsilon_\gamma}{\varepsilon_\omega + \varepsilon_\gamma} + \frac{\alpha}{\mathcal{K}} \frac{\varepsilon_\omega}{\varepsilon_\omega + \varepsilon_\gamma} \langle s_\omega \rangle^\omega - \frac{\alpha}{\mathcal{K}} s_\omega. \tag{44}$$

Problem II (b-problem)

$$\begin{aligned} \mathbf{v}_\gamma \cdot \nabla \mathbf{b}_\gamma = {} & \nabla \cdot \left(\mathbf{D}_\gamma \cdot \nabla \mathbf{b}_\gamma \right) - \tilde{\mathbf{v}}_\gamma - \frac{\varepsilon_\omega}{\varepsilon_\omega + \varepsilon_\gamma} \left\langle \mathbf{v}_\gamma \right\rangle^\gamma - \frac{\alpha}{\mathcal{K}} \frac{\varepsilon_\gamma}{\varepsilon_\omega + \varepsilon_\gamma} \left\langle \mathbf{b}_\gamma \right\rangle^\gamma \\ & + \frac{\varepsilon_\omega}{\varepsilon_\gamma + \varepsilon_\omega} \mathbf{D}_\omega \cdot \langle \nabla s_\omega \rangle^\omega + \frac{\varepsilon_\gamma}{\varepsilon_\gamma + \varepsilon_\omega} \mathbf{D}_a \cdot \left\langle \nabla s_\gamma \right\rangle^\gamma - 2\mathbf{D}_\gamma \cdot \nabla s_\gamma \\ & + \mathbf{v}_\gamma s_\gamma - \frac{\varepsilon_\gamma}{\varepsilon_\omega + \varepsilon_\gamma} \left\langle s_\gamma \mathbf{v}_\gamma \right\rangle^\gamma \end{aligned} \tag{45}$$

$$BC1: \quad -\left(\mathbf{n}_{\gamma\sigma} \cdot \mathbf{D}_\gamma \right) \cdot \nabla \mathbf{b}_\gamma = \left(\mathbf{n}_{\gamma\sigma} \cdot \mathbf{D}_\gamma \right) \left(1 - s_\gamma \right) \qquad \text{on } \mathcal{S}_{\gamma\sigma} \tag{46a}$$

$$BC2: \quad \mathbf{b}_\omega = \mathbf{b}_\gamma \qquad \text{on } \mathcal{S}_{\gamma\omega} \tag{46b}$$

$$BC3: \quad -\mathbf{n}_{\gamma\omega} \cdot \left(\mathbf{D}_\gamma \cdot \nabla \mathbf{b}_\gamma - \mathbf{D}_\omega \cdot \nabla \mathbf{b}_\omega \right) = -\mathbf{n}_{\gamma\omega} \cdot \left(\mathbf{D}_\omega - \mathbf{D}_\gamma \right) \left(1 - s_\gamma \right) \quad \text{on } \mathcal{S}_{\gamma\omega} \tag{46c}$$

$$BC4: \quad -(\mathbf{n}_{\omega\sigma} \cdot \mathbf{D}_\omega) \cdot \nabla \mathbf{b}_\omega = (\mathbf{n}_{\omega\sigma} \cdot \mathbf{D}_\omega)(1 - s_\omega) \qquad \text{on } \mathcal{S}_{\omega\sigma} \tag{46d}$$

$$\begin{aligned} 0 = {} & \nabla \cdot (\mathbf{D}_\omega \cdot \nabla \mathbf{b}_\omega) + \frac{\varepsilon_\gamma}{\varepsilon_\gamma + \varepsilon_\omega} \left\langle \mathbf{v}_\gamma \right\rangle^\gamma + \frac{\alpha}{\mathcal{K}} \frac{\varepsilon_\omega}{\varepsilon_\omega + \varepsilon_\gamma} \langle \mathbf{b}_\omega \rangle^\omega - \frac{\alpha}{\mathcal{K}} \mathbf{b}_\omega \\ & + \frac{\varepsilon_\omega}{\varepsilon_\gamma + \varepsilon_\omega} \mathbf{D}_\omega \cdot \langle \nabla s_\omega \rangle^\omega + \frac{\varepsilon_\gamma}{\varepsilon_\gamma + \varepsilon_\omega} \mathbf{D}_\gamma \cdot \left\langle \nabla s_\gamma \right\rangle^\gamma - 2\mathbf{D}_\omega \cdot \nabla s_\omega \\ & - \frac{\varepsilon_\gamma}{\varepsilon_\omega + \varepsilon_\gamma} \left\langle s_\gamma \mathbf{v}_\gamma \right\rangle^\gamma. \end{aligned} \tag{47}$$

The mathematical procedure carried out for the development of these two boundary value problems leads to a coupling between both closure parameters. For example, the quantity $\mathbf{v}_\gamma s_\gamma$ appears in Eq. (45). Such terms, connecting the closure parameters associated with different orders of derivatives of the macroscopic concentrations, are not classical in the volume averaging method and are usually neglected, especially for the development of the so-called two-equation models. It has been proven that this coupling is necessary when solving the classical Graetz problem [52]. However, whether this additional feature leads to a better description of the mass transport in disordered porous media, or whether this should be neglected is still a matter of debates.

4.3. Closure assumptions

There is an interesting discussion concerning the concept of representative elementary volume (REV) which is often misunderstood. Within hierarchical porous media, there is substantial redundancy in the spatial structure of the transport processes at the microscale, that is, the information needed to calculate the effective parameters is contained in a relatively small representative portion of the medium. Within this REV, internal boundary conditions, say Eq. (46a) for example, between the different phases are determined by the physics at the pore-scale. However, in order to ensure unicity of the s and $\mathbf{b}$ fields, it is also mandatory to adopt a representation for the external boundary condition between the REV and the rest of the porous medium. This condition is not determined by the physics at the pore-scale but rather represents a way of closing the problem. At first, it is unclear how this choice should be made and it results in a significant amount of confusion in the literature. From a theoretical point of view, if the REV is large enough (read if the hypothesis of separation of length scales is verified), it has been shown [27] that effective parameters do not depend on this boundary condition.

In the real world, this constraint is never exactly satisfied, that is, the boundary condition influences the microscopic fields and the effective parameters. However, it is important to notice that in the macroscopic Eq. (29), $\hat{c}$ appears only under integrated quantities. Because of this, the dependence of effective parameters upon the solution of the closure problem is essentially mathematically of a weak form [53]. Hence, one could choose, say, Dirichlet, Neumann, mixed or periodic boundary conditions to obtain a local solution which produces acceptable values for the associated averaged quantities. As previously discussed in the literature [54–58], the periodic boundary condition lends itself very well for this application as it induces very little perturbation in the local fields, in opposition to, say, Dirichlet boundary conditions. It must be understood that this does not mean that the medium is interpreted as being physically periodic. For the remainder of this work, we will assume that the medium can be represented locally by a periodic cell Eq. (48) and that the effective parameters can be calculated over this representative part of the medium.

$$\text{Periodicity}: \quad \hat{c}_i(\mathbf{x} + l_k) = \hat{c}_i(\mathbf{x}) \quad k = x, y, z. \tag{48}$$

We also have Eqs. (49) and (50)

$$\text{Periodicity}: \quad \mathbf{b}_i(\mathbf{x} + l_k) = \mathbf{b}_i(\mathbf{x}) \quad k = x, y, z \tag{49}$$

$$\text{Periodicity}: \quad s_i(\mathbf{x} + l_k) = s_i(\mathbf{x}) \quad k = x, y, z. \tag{50}$$

In these Eqs. (48)–(50), we have used l_k to represent the three lattice vectors that are needed to describe the 3-D spatial periodicity.

In addition to these periodic boundary conditions, one usually needs to impose constraints on the intrinsic averaged of the closure fields in order to ensure unicity of the solutions. To find out these additional equations, we use $\langle \tilde{c}_\gamma \rangle^\gamma, \langle \tilde{c}_\omega \rangle^\omega = 0$. In our case, this is not necessary to

constrain the fields because the reactive part of the spatial operator ensures, mathematically, unicity of the solutions. However, numerical computations, in situations where the reaction has little importance in comparison to other processes, can lead to some discrepancies. To avoid this problem, it is important to impose $\varepsilon_\omega \langle \hat{c}_\omega \rangle^\omega + \varepsilon_\gamma \langle \hat{c}_\gamma \rangle^\gamma = 0$, that is, $\varepsilon_\omega \langle \mathbf{b}_\omega \rangle^\omega + \varepsilon_\gamma \langle \mathbf{b}_\gamma \rangle^\gamma = 0$ and $\varepsilon_\omega \langle s_\omega \rangle^\omega + \varepsilon_\gamma \langle s_\gamma \rangle^\gamma = 0$.

4.4. Closed macroscopic equation

Substituting Eqs. (40) and (41) into Eq. (29) leads to

$$\frac{\partial \langle c \rangle^{\gamma\omega}}{\partial t} + \mathbf{v}^* \cdot \nabla \langle c \rangle^{\gamma\omega} = \nabla \cdot \left(\mathbf{D}^* \cdot \nabla \langle c \rangle^{\gamma\omega} \right) - \alpha^* \langle c \rangle^{\gamma\omega} \tag{51}$$

where the effective parameters are given by

$$\mathbf{v}^* = \frac{\varepsilon_\gamma}{\varepsilon_\gamma + \varepsilon_\omega} \left(\langle \mathbf{v}_\gamma \rangle^\gamma + \mathbf{D}_\gamma \cdot \langle \nabla s_\gamma \rangle^\gamma - \langle s_\gamma \mathbf{v}_\gamma \rangle^\gamma \right) + \frac{\varepsilon_\omega}{\varepsilon_\gamma + \varepsilon_\omega} \left(\mathbf{D}_\omega \cdot \langle \nabla s_\omega \rangle^\omega + \frac{\alpha}{\mathcal{K}} \langle \mathbf{b}_\omega \rangle^\omega \right) \tag{52}$$

$$\mathbf{D}^* = \frac{\varepsilon_\gamma}{\varepsilon_\gamma + \varepsilon_\omega} \left[\mathbf{D}_\gamma \cdot \left(\mathbf{I} - \mathbf{I} \langle s_\gamma \rangle^\gamma + \langle \nabla \mathbf{b}_\gamma \rangle^\gamma \right) - \langle \mathbf{v}_\gamma \mathbf{b}_\gamma \rangle^\gamma \right] + \frac{\varepsilon_\omega}{\varepsilon_\gamma + \varepsilon_\omega} \left[\mathbf{D}_\omega \cdot \left(\mathbf{I} - \mathbf{I} \langle s_\omega \rangle^\omega + \langle \nabla \mathbf{b}_\omega \rangle^\omega \right) \right] \tag{53}$$

$$\alpha^* = \frac{\alpha}{\mathcal{K}} \frac{\varepsilon_\omega}{\varepsilon_\gamma + \varepsilon_\omega} \left(1 - \langle s_\omega \rangle^\omega \right). \tag{54}$$

For simplicity, the volumic fractions are taken to be constants. If the model is applied to media with non constant porosities, one should take care to consider gradients of ε (c.f., Appendixes). Moreover, the macroscopic equation is written under a non-conservative form so that it exhibits only effective velocity, dispersion and effective reaction rate. It is convenient to write it this way for the purpose of comparing the asymptotic model with other models.

However, a more general conservative expression would be

$$\frac{\partial \langle c \rangle^{\gamma\omega}}{\partial t} + \nabla \cdot \left(\frac{\varepsilon_\gamma}{\varepsilon_\gamma + \varepsilon_\omega} \langle c \rangle^{\gamma\omega} \langle \mathbf{v}_\gamma \rangle^\gamma \right) = \nabla \cdot \left(\mathbf{D}_c^* \cdot \nabla \langle c \rangle^{\gamma\omega} \right) - \nabla \cdot \left(\mathbf{d}_c^* \langle c \rangle^{\gamma\omega} \right) - \mathbf{v}_c^* \cdot \nabla \langle c \rangle^{\gamma\omega} - \alpha_c^* \langle c \rangle^{\gamma\omega} \tag{55}$$

where the effective parameters are given by

$$\mathbf{d}_c^* = \frac{\varepsilon_\gamma}{\varepsilon_\gamma + \varepsilon_\omega} \left(\mathbf{D}_\gamma \cdot \langle \nabla s_\gamma \rangle^\gamma - \langle s_\gamma \mathbf{v}_\gamma \rangle^\gamma \right) + \frac{\varepsilon_\omega}{\varepsilon_\gamma + \varepsilon_\omega} \left(\mathbf{D}_\omega \cdot \langle \nabla s_\omega \rangle^\omega \right) \tag{56}$$

$$\mathbf{v}_c^* = \frac{\varepsilon_\omega}{\varepsilon_\gamma + \varepsilon_\omega} \frac{\alpha}{\mathcal{K}} \langle \mathbf{b}_\omega \rangle^\omega \tag{57}$$

$$\mathbf{D}_c^* = \frac{\varepsilon_\gamma}{\varepsilon_\gamma + \varepsilon_\omega} \left[\mathbf{D}_\gamma \cdot \left(\mathbf{I} - \mathbf{I} \langle s_\gamma \rangle^\gamma + \langle \nabla \mathbf{b}_\gamma \rangle^\gamma \right) - \langle \mathbf{v}_\gamma \mathbf{b}_\gamma \rangle^\gamma \right] + \frac{\varepsilon_\omega}{\varepsilon_\gamma + \varepsilon_\omega} \left[\mathbf{D}_\omega \cdot \left(\mathbf{I} - \mathbf{I} \langle s_\omega \rangle^\omega + \langle \nabla \mathbf{b}_\omega \rangle^\omega \right) \right] \tag{58}$$

$$\alpha_c^* = \frac{\alpha}{\mathcal{K}} \frac{\varepsilon_\omega}{\varepsilon_\gamma + \varepsilon_\omega} \left(1 - \langle s_\omega \rangle^\omega \right). \tag{59}$$

At this point, if $\mathbf{v}_c^*$ plays mathematically the role of a velocity, it is directly linked to the chemical reaction and should not be discarded if one considers non-convective flows.

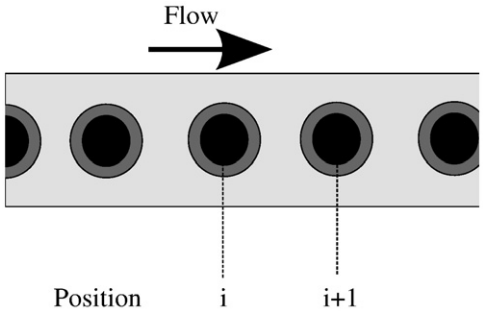

Fig. 3. Total geometry.

5. Numerical results

Ideally, one could compare the theory developed above with the results of direct experimental measurements conducted at both the microscale and at the macroscale. Theoretically, it is possible to obtain a three dimensional image of the three phases biofilm–liquid–solid. This is an area of active research [59], and workers are continuing to develop methods such that the microscale structure of a biofilm within a porous medium can be measured [60,61]. Currently, however, the results from such multi-scale experimental measurements are not available. The goal of this section, then, is to provide some characteristic features of the model previously devised on a simplified 2D medium Figs. 3 and 4 using numerical methods.

We adopt a conceptual construction which captures the main physics of the problem. In Fig. 4, σ-phase is represented by solid black, the γ-phase is given by light grey, and the grey lies for the ω-phase. One should notice that at the macroscale only a 1D model is needed for this particular geometry. For both the 2D and 1D models, the output boundary condition is set to free advective flux. For the purposes of this study, 1) we obtain the velocity field by solving Stokes equations, with no-slip conditions on lateral boundaries, over the entire system, 2) we will only consider a spheric diffusion tensor for the biofilm and water-phases, 3) we fix $\mathcal{K} = 0.5$ and $D_\Sigma = \frac{D_\omega}{D_\gamma} = 0.3$ and take $l_\gamma = 0.5$. Numerical calculations were performed using the COMSOL™ Multiphysics package 3.5 based on a finite element formulation. For the resolution of Stokes equation, we use quadratic Lagrange elements for the velocities and linear for the pressure. For the resolution of the advection–diffusion equations, we use a quadratic Lagrange element formulation. Residuals are computed using a quadrature formula of order 2 for linear Lagrange elements and 4 for quadratic Lagrange elements. The linear systems

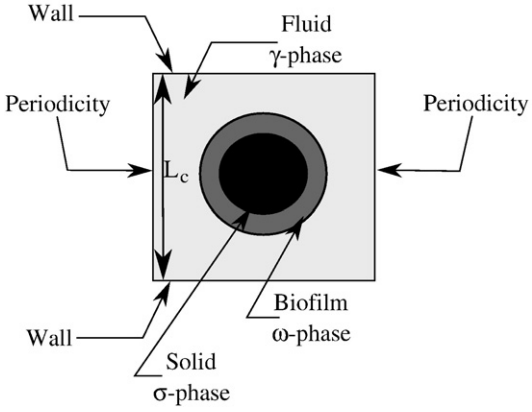

Fig. 4. Representative cell.

are solved using the direct solver UMFPACK based on the Unsymmetric MultiFrontal method. Mesh convergence was carefully examined for each computation.

For these simulations, we have the following precise goals

1. To establish the behavior of the effective parameters as functions of Péclet and Damköhler numbers.
2. To compare these effective parameters with those of the local mass equilibrium model, as developed in [26].
3. To validate the model against pore-scale simulations both stationary and transient.

The problem Eqs. (5)–(7) at the pore-scale can be rewritten under the following dimensionless form

$$\gamma\text{–phase}: \quad \frac{\partial c_\gamma^{'}}{\partial t^{'}} + \mathcal{P}e\nabla\cdot\left(c_\gamma^{'}\mathbf{v}^{'}{}_\gamma\right) = \Delta c_\gamma^{'} \tag{60}$$

$$BC1: \quad -\mathbf{n}_{\gamma\sigma}\cdot\nabla c_\gamma^{'} = 0 \qquad \text{on } \mathcal{S}_{\gamma\sigma} \tag{61a}$$

$$BC2: \quad c_\omega^{'} = c_\gamma^{'} \qquad \text{on } \mathcal{S}_{\gamma\omega} \tag{61b}$$

$$BC3: \quad -\mathbf{n}_{\gamma\omega}\cdot\nabla c_\gamma^{'} = -\mathrm{D}_\Sigma\mathbf{n}_{\gamma\omega}\cdot\nabla c_\omega^{'} \qquad \text{on } \mathcal{S}_{\gamma\omega} \tag{61c}$$

$$BC4: \quad -\mathrm{D}_\Sigma\mathbf{n}_{\omega\sigma}\cdot\nabla c_\omega^{'} = 0 \qquad \text{on } \mathcal{S}_{\omega\sigma} \tag{61d}$$

$$\omega\text{–phase}: \quad \frac{\partial c_\omega^{'}}{\partial t^{'}} = \nabla\cdot\left(D_\Sigma\nabla c_\omega^{'}\right) - \mathcal{D}aD_\Sigma c_\omega^{'} \tag{62}$$

where the normalized concentrations and velocity are given by

$$c_\omega^{'} = \frac{c_\omega}{c_0} \tag{63}$$

$$c_\gamma^{'} = \frac{c_\gamma}{c_0} \tag{64}$$

$$v_\gamma^{'} = \frac{v_y}{\langle v_\gamma\rangle^\gamma}. \tag{65}$$

The concentration c_0 is the amplitude of the input concentration. Notice that we impose $c_0 \ll \mathcal{K}$ which is a sufficient constraint for the linearization of the reaction rate. We have adopted the following additional definitions for dimensionless quantities

$$t^{'} = \frac{t\langle v_\gamma\rangle^\gamma}{l_\gamma}. \tag{66}$$

The ratio between the diffusion coefficients in the ω-phase and γ-phase is

$$D_\Sigma = \frac{D_\omega}{D_\gamma}. \tag{67}$$

The Péclet and Damköhler numbers are specified by

$$\mathcal{D}a = \frac{\alpha l_\gamma^2}{\mathcal{K}D_\omega} \tag{68}$$

$$\mathcal{P}e = \frac{\langle v_\gamma\rangle^\gamma l_\gamma}{D_\gamma}. \tag{69}$$

The closure problems Eqs. (42)–(47) take the form in dimensionless quantities

Problem I (s-problem)

$$\mathcal{P}e\nabla\cdot\left(\mathbf{v}_\gamma^{'}s_\gamma\right) = \Delta s_\gamma - \mathcal{D}a\frac{\varepsilon_\omega}{\varepsilon_\omega+\varepsilon_\gamma} - \mathcal{D}a\frac{\varepsilon_\gamma}{\varepsilon_\omega+\varepsilon_\gamma}\langle s_\gamma\rangle^\gamma \tag{70}$$

$$BC1: \quad -\mathbf{n}_{\gamma\sigma}\cdot\nabla s_\gamma = 0 \qquad \text{on } \mathcal{S}_{\gamma\sigma} \tag{71a}$$

$$BC2: \quad s_\omega = s_\gamma \qquad \text{on } \mathcal{S}_{\gamma\omega} \tag{71b}$$

$$BC3: \quad -\mathbf{n}_{\gamma\omega}\cdot\nabla s_\gamma = -\mathrm{D}_\Sigma\mathbf{n}_{\gamma\omega}\cdot\nabla s_\omega \qquad \text{on } \mathcal{S}_{\gamma\omega} \tag{71c}$$

$$BC4: \quad -\mathrm{D}_\Sigma\mathbf{n}_{\omega\sigma}\cdot\nabla s_\omega = 0 \qquad \text{on } \mathcal{S}_{\omega\sigma} \tag{71d}$$

$$\text{Periodicity}: \quad s_i(\mathbf{x}+l_x) = s_i(\mathbf{x}) \tag{71e}$$

$$0 = \nabla\cdot(\mathrm{D}_\Sigma\nabla s_\omega) + \mathcal{D}a\frac{\varepsilon_\gamma}{\varepsilon_\omega+\varepsilon_\gamma} + \mathcal{D}a\frac{\varepsilon_\omega}{\varepsilon_\omega+\varepsilon_\gamma}\langle s_\omega\rangle^\omega - \mathcal{D}as_\omega. \tag{72}$$

Problem II (b-problem)

$$\begin{aligned}\mathcal{P}e\left(\mathbf{v}_\gamma^{'}\cdot\nabla\mathbf{b}_\gamma^{'} - \mathbf{v}_\gamma^{'}s_\gamma + \tilde{\mathbf{v}}_\gamma^{'}\right) = \nabla\cdot\left(\nabla\mathbf{b}_\gamma^{'}\right) - 2\nabla s_\gamma - \mathcal{D}a\frac{\varepsilon_\gamma}{\varepsilon_\omega+\varepsilon_\gamma}\left\langle\mathbf{b}^{'}{}_\gamma\right\rangle^\gamma \\ - \frac{\mathcal{P}e}{\varepsilon_\omega+\varepsilon_\gamma}\left\langle s_\gamma\mathbf{v}_\gamma^{'}\right\rangle + \frac{\varepsilon_\omega}{\varepsilon_\gamma+\varepsilon_\omega}\mathrm{D}_\Sigma\langle\nabla s_\omega\rangle^\omega \\ + \frac{\varepsilon_\gamma}{\varepsilon_\gamma+\varepsilon_\omega}\left\langle\nabla s_\gamma\right\rangle^\gamma\end{aligned} \tag{73}$$

$$BC1: \quad -\mathbf{n}_{\gamma\sigma}\cdot\nabla\mathbf{b}_\gamma^{'} = \mathbf{n}_{\gamma\sigma}\left(1-s_\gamma\right) \qquad \text{on } \mathcal{S}_{\gamma\sigma} \tag{74a}$$

$$BC2: \quad \mathbf{b}_\omega^{'} = \mathbf{b}_\gamma^{'} \qquad \text{on } \mathcal{S}_{\gamma\omega} \tag{74b}$$

$$BC3: \quad -\mathbf{n}_{\gamma\omega}\cdot\left(\nabla\mathbf{b}_\gamma^{'} - \mathrm{D}_\Sigma\nabla\mathbf{b}_\omega^{'}\right) = -\mathbf{n}_{\gamma\omega}(\mathrm{D}_\Sigma-1)\left(1-s_\gamma\right) \qquad \text{on } \mathcal{S}_{\gamma\omega} \tag{74c}$$

$$BC4: \quad -\mathbf{n}_{\omega\sigma}\cdot\nabla\mathbf{b}_\omega^{'} = \mathbf{n}_{\omega\sigma}(1-s_\omega) \qquad \text{on } \mathcal{S}_{\omega\sigma} \tag{74d}$$

$$\textit{Periodicity}: \quad \mathbf{b}_i^{'}(\mathbf{x}+l_x) = \mathbf{b}_i^{'}(\mathbf{x}) \tag{74e}$$

$$\begin{aligned}0 = \nabla\cdot\left(\mathrm{D}_\Sigma\nabla\mathbf{b}_\omega^{'}\right) - 2\mathrm{D}_\Sigma\nabla s_\omega + \mathcal{D}a\frac{\varepsilon_\omega}{\varepsilon_\omega+\varepsilon_\gamma}\left\langle\mathbf{b}_\omega^{'}\right\rangle^\omega - \mathcal{D}a\mathbf{b}_\omega^{'} \\ - \frac{\mathcal{P}e}{\varepsilon_\omega+\varepsilon_\gamma}\left\langle s_\gamma\mathbf{v}_\gamma^{'}\right\rangle + \frac{\varepsilon_\omega}{\varepsilon_\gamma+\varepsilon_\omega}\mathrm{D}_\Sigma\langle\nabla s_\omega\rangle^\omega + \frac{\varepsilon_\gamma}{\varepsilon_\gamma+\varepsilon_\omega}\left\langle\nabla s_\gamma\right\rangle^\gamma\end{aligned} \tag{75}$$

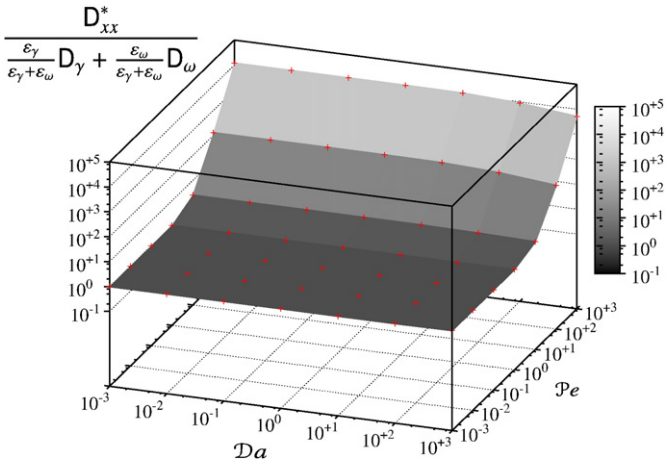

Fig. 5. Normalized longitudinal dispersion of the non-equilibrium model as a function of $\mathcal{P}e$ and $\mathcal{D}a$ numbers.

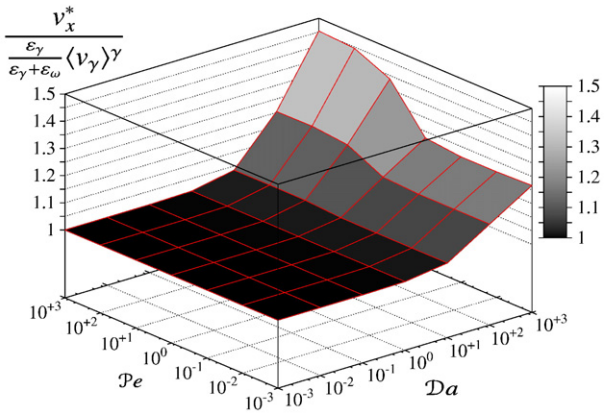

Fig. 6. Normalized x-component of the effective velocity of the non-equilibrium model as a function of $\mathcal{P}e$ and $\mathcal{D}a$ numbers.

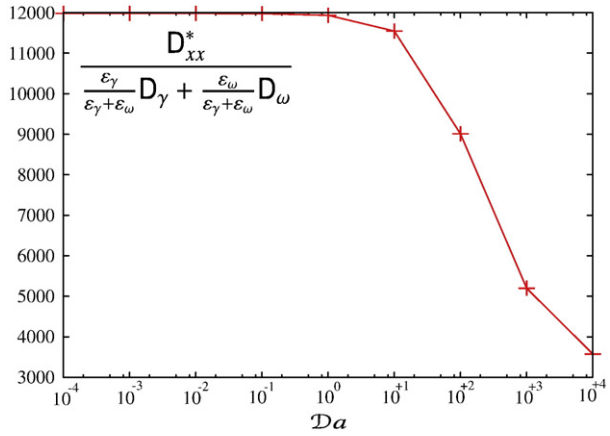

Fig. 8. Normalized dispersion behavior of the non-equilibrium model for $\mathcal{P}e = 1000$ as a function of $\mathcal{D}a$ number.

where

$$\tilde{\mathbf{v}}_\gamma' = \frac{\tilde{\mathbf{v}}_\gamma}{\langle v_\gamma \rangle^\gamma} \quad \mathbf{b}_\gamma' = \frac{\mathbf{b}_\gamma}{l_\gamma} \quad \mathbf{b}_\omega' = \frac{\mathbf{b}_\omega}{l_\gamma}. \tag{76}$$

Notice that, if one fixes D_Σ, the set of equations only depends upon $\mathcal{P}e$ and $\mathcal{D}a$.

5.1. Effective velocity, dispersion and reactive behavior

In this section, we solve the closure parameter problems (70)–(75) over the cell Fig. 4 for large ranges of $\mathcal{P}e$ and $\mathcal{D}a$. Then, the associated effective parameters are computed and presented Fig. 5 for the longitudinal dispersion D_{xx}^* normalized with $\frac{\varepsilon_\gamma}{\varepsilon_\gamma+\varepsilon_\omega}D_\gamma + \frac{\varepsilon_\omega}{\varepsilon_\gamma+\varepsilon_\omega}D_\omega$; Fig. 6 for the x-component of the effective velocity v_x^* normalized with $\frac{\varepsilon_\gamma}{\varepsilon_\gamma+\varepsilon_\gamma}\langle v_\gamma\rangle^\gamma$; Fig. 7 for the effective kinetics α normalized with $\frac{\varepsilon_\omega}{\varepsilon_\gamma+\varepsilon_\gamma}\frac{\alpha}{\mathcal{K}}$. For low $\mathcal{P}e$ and high $\mathcal{D}a$, the length scale constraints needed to develop the closed macroscopic equation are not satisfied. However, the constraints previously developed are expressed in terms of order of magnitudes so that it is not clear what is the exact limit between the homogenizable and non-homogenizable zones. Because of this, the entire space of $\mathcal{P}e$, $\mathcal{D}a$ parameter is kept and we do not clearly establish this frontier.

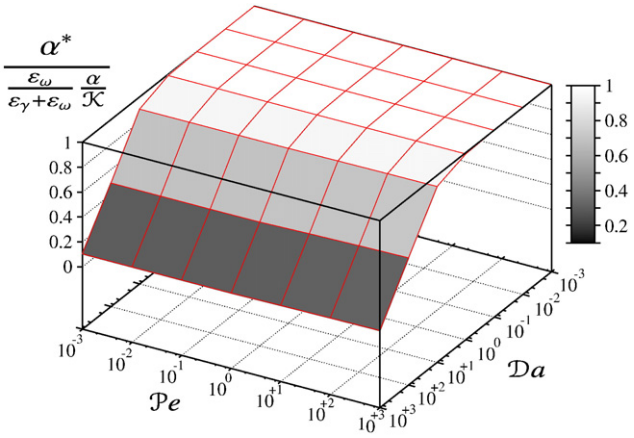

Fig. 7. Normalized effective reaction rate of the non-equilibrium model as a function of $\mathcal{P}e$ and $\mathcal{D}a$ numbers.

5.1.1. Velocity

Effective parameters strongly depend upon the type of boundary conditions at the small scale, that is, the dispersion in a, say, Dirichlet bounded system or in a Neumann bounded problem may drastically change. In our case, for low $\mathcal{D}a$, the boundary between the biofilm-phase and the fluid-phase is a flux continuity whereas, as $\mathcal{D}a$ tends toward infinity, the concentration in the biofilm-phase and at the boundary tends toward zero, which can be interpreted, for conceptual purposes, as a Dirichlet boundary condition. In other words, when $\mathcal{P}e \gg 1$ and $\mathcal{D}a \gg 1$ the medium can conceptually be represented by a zero-concentration layer surrounding the biofilm, that is, the substrate reaches a limited interstitial space corresponding to the maxima of the local velocity field. It results in an increase of the apparent velocity with both $\mathcal{P}e$ and $\mathcal{D}a$ numbers.

5.1.2. Dispersion

The dispersion exhibits the classical form, and increases mainly with the $\mathcal{P}e$ number as the hydrodynamic dispersion becomes predominant. However, the log scale hides the fact that D^* actually depends also on $\mathcal{D}a$ and this is presented in Fig. 8. We observe a drastic reduction of the longitudinal dispersion at high $\mathcal{D}a$ and it is in agreement with previous studies [40,62,63]. The physics underlying this effect is reminiscent to the one causing an augmentation of the apparent velocity. As a boundary layer in which $c_\gamma = 0$ surrounds the biofilm-phase, the solute is confined in a small portion of the fluid-phase or, more precisely, undertakes biodegradation as soon as it reaches the edges of this zone. The molecules of solute far away from the entrance have not visited the entire γ-phase but rather a narrow central portion in which the fluctuations of the velocity field are limited. As a consequence, the substrate spreading due to hydrodynamic dispersion (reminiscent to the Taylor dispersion in a tube) is reduced. Additionally, it is important to keep in mind that our model porous medium does not exhibit any transverse dispersion. If it was to be considered, one would expect a different behavior for the transverse dispersion (see discussions in [40,62,63]).

5.1.3. Effectiveness factor

The effective reaction rate depends almost only on $\mathcal{D}a$ because the mass transfer through the boundary is mainly driven by diffusion. It seems that, for low $\mathcal{D}a$, the reaction rate is maximum and decreases when the consumption is too elevated compared to diffusion. It suggests that the reaction rate could be written under the form ηR_{max} with $\eta \leq 1$ a function of $\mathcal{D}a$. Notice that Dykaar and Kitanidis [40], following the work of Shapiro [63] for a surface reactive medium, also established a theoretical framework for this kind of effectiveness factor using the moments matching technique. However, their model describes an averaged concentration only on the water-phase rather than the total mass present in the porous medium at a given time. The

reader is referred to the Section 3.3 for an extensive discussion of this point.

5.2. Relationship with the local mass equilibrium model

In this part, we compare the local mass equilibrium model as developed in [26] with the non-equilibrium one-equation model. The local mass equilibrium model takes the form

$$\frac{\partial \langle c\rangle^{\gamma\omega}}{\partial t} + \mathbf{v}^{*}_{Equ}\cdot\nabla\langle c\rangle^{\gamma\omega} = \nabla\cdot\left(\mathbf{D}^{*}_{Equ}\cdot\nabla\langle c\rangle^{\gamma\omega}\right) - \alpha^{*}_{Equ}\langle c\rangle^{\gamma\omega} \tag{77}$$

where the effective parameters are given by

$$\mathbf{v}^{*}_{Equ} = \frac{\varepsilon_\gamma}{\varepsilon_\gamma+\varepsilon_\omega}\left\langle \mathbf{v}_\gamma\right\rangle^{\gamma} \tag{78}$$

$$\mathbf{D}^{*}_{Equ} = \frac{\varepsilon_\gamma}{\varepsilon_\gamma+\varepsilon_\omega}\left[\mathrm{D}_\gamma\left\langle\nabla\mathbf{b}_{\gamma Equ}\right\rangle^{\gamma}\right] + \frac{\varepsilon_\omega}{\varepsilon_\gamma+\varepsilon_\omega}\left[\mathrm{D}_\omega\left\langle\nabla\mathbf{b}_{\gamma Equ}\right\rangle^{\gamma}\right] - \frac{1}{\varepsilon_\gamma+\varepsilon_\omega}\left\langle\tilde{\mathbf{v}}_\gamma\mathbf{b}_{\gamma Equ}\right\rangle \tag{79}$$

$$\alpha^{*}_{Equ} = \frac{\alpha}{\mathcal{K}}\frac{\varepsilon_\omega}{\varepsilon_\gamma+\varepsilon_\omega}. \tag{80}$$

The closure parameters are solutions of the following problem

$$\gamma\text{–phase}: \quad \mathcal{P}e\left(\mathbf{v}'_\gamma\cdot\nabla\mathbf{b}'_{\gamma Equ} + \tilde{\mathbf{v}}'_\gamma\right) = \nabla\cdot\left(\nabla\mathbf{b}'_{\gamma Equ}\right) \tag{81}$$

$$BC1: \quad -\mathbf{n}_{\gamma\sigma}\cdot\nabla\mathbf{b}'_{\gamma Equ} = \mathbf{n}_{\gamma\sigma} \quad \text{on } \mathcal{S}_{\gamma\sigma} \tag{82a}$$

$$BC2: \quad \mathbf{b}'_{\omega Equ} = \mathbf{b}'_{\gamma Equ} \quad \text{on } \mathcal{S}_{\gamma\omega} \tag{82b}$$

$$BC3: \quad -\mathbf{n}_{\gamma\omega}\cdot\left(\nabla\mathbf{b}'_\gamma - \mathrm{D}_\Sigma\nabla\mathbf{b}'_{\omega Equ}\right) = -\mathbf{n}_{\gamma\omega}(\mathrm{D}_\Sigma - 1) \quad \text{on } \mathcal{S}_{\gamma\omega} \tag{82c}$$

$$BC4: \quad -\mathbf{n}_{\omega\sigma}\cdot\nabla\mathbf{b}'_{\omega Equ} = \mathbf{n}_{\omega\sigma} \quad \text{on } \mathcal{S}_{\omega\sigma} \tag{82d}$$

$$Periodicity: \quad \mathbf{b}'_{iEqu}(\mathbf{x}+l_x) = \mathbf{b}'_{iEqu}(\mathbf{x}) \tag{82e}$$

$$\omega\text{–phase}: \quad 0 = \nabla\cdot\left(\mathrm{D}_\Sigma\nabla\mathbf{b}'_{\omega Equ}\right) - \mathcal{D}a\mathbf{b}'_{\omega Equ} \tag{83}$$

where

$$\mathbf{b}'_{\gamma Equ} = \frac{\mathbf{b}_{\gamma Equ}}{l_\gamma} \quad \mathbf{b}'_{\omega Equ} = \frac{\mathbf{b}_{\omega Equ}}{l_\gamma}. \tag{84}$$

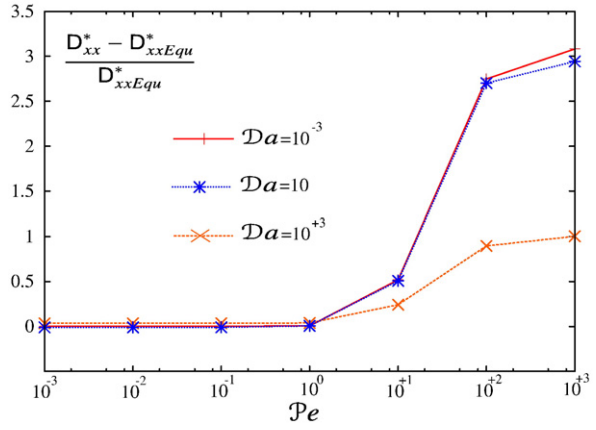

Fig. 9. Relative differences of the longitudinal dispersion between local mass equilibrium and non-equilibrium models as functions of $\mathcal{P}e$ for different $\mathcal{D}a$ numbers.

In the local mass equilibrium model, the effective reaction rate and velocity are constant in terms of $\mathcal{P}e$ and $\mathcal{D}a$ numbers. Notice that, on Fig. 6 and Fig. 7 the effective parameters of the non-equilibrium model are directly normalized with those of the equilibrium one. Because of this, the comparison is straightforward and both are close to each other for $\mathcal{D}a \leq 1$.

For the dispersion, the relative difference between both models, in terms of $\mathcal{P}e$ and $\mathcal{D}a$ numbers, is presented in Fig. 9. For $\mathcal{P}e \leq 1$, the relative difference is close to zero so that both models are equivalent for $\mathcal{D}a \leq 1$ and $\mathcal{P}e \leq 1$. It has been shown in [26] that this region of the $\mathcal{D}a$, $\mathcal{P}e$ space represents the entire region of validity of the local mass equilibrium model. As a direct consequence, it turns out that the non-equilibrium model includes the equilibrium one when this one is valid. A thorough study of the transient behavior for both models is performed and discussed in the next section.

5.3. Comparison with direct numerical simulation

The aim of this section is to provide direct evidences that the model allows a good approximation of the situation at the pore-scale, to catch its limits and to study some physics of the problem. On the one hand, we solve the entire 2D microscopic problem on a total length of $120L_c$ (called DNS for direct numerical simulation). On the other hand, we solve the 1D upscaled models on a total length of $120L_c$. First, we observe the stationary response of the system for different Péclet and Damköhler numbers. Both boundary conditions at the output are free advective flux. Then, we study the breakthrough curves at $20L_c$, $60L_c$ and $100L_c$ for a square input of a width of $\delta t' = 5$ starting at $t' = 0$ for different Péclet and Damköhler numbers.

5.3.1. Stationary analysis

The comparison of the concentration fields between the DNS and the non-equilibrium model is presented Fig. 10 for $\mathcal{P}e = 10$, $\mathcal{D}a = 10$; Fig. 11 for $\mathcal{P}e = 100$, $\mathcal{D}a = 100$ and Fig. 12 for $\mathcal{P}e = 1000$, $\mathcal{D}a = 1000$. Each circle, cross and square represents the value of $\langle c\rangle^{\gamma\omega}$ integrated on a cell. We solve the stationary boundary value problem Eqs. (5)–(7) with an input Dirichlet boundary condition of amplitude c_0. Then the results are normalized using the value of $\langle c\rangle^{\gamma\omega}$ calculated on the first cell (DNSB) and on the cell number 20 (DNSA) for Fig. 10 and Fig. 11; and on the first cell (DNSB), on the cell number 20 (DNSA) and 40 (DNSC). The origin of the spatial base is modified consequently to make them all start at 0.

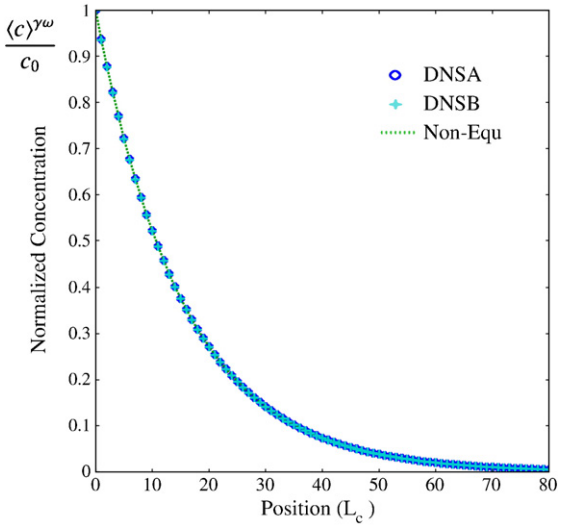

Fig. 10. DNS and non-equilibrium model stationary concentration fields for $\mathcal{P}e = 10$ and $\mathcal{D}a = 10$ using normalization on the first cell (DNSB) and on the cell number 20 (DNSA).

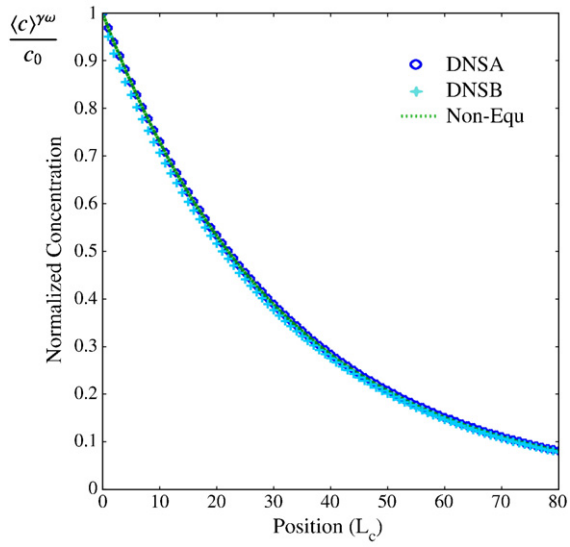

Fig. 11. DNS and non-equilibrium model stationary concentration fields for $\mathcal{P}e = 100$ and $\mathcal{D}a = 100$ using normalization on the first cell (DNSB) and on the cell number 20 (DNSA).

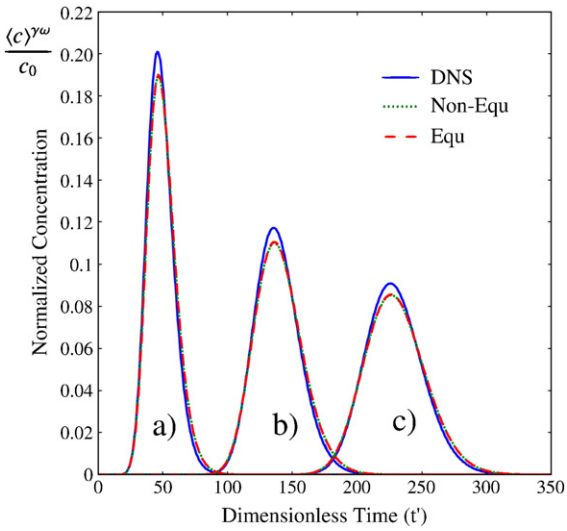

Fig. 13. Transient breakthrough curves for the DNS, the local non-equilibrium and equilibrium models for a square input of $\delta t' = 5$ for $\mathcal{P}e = 1$ and $\mathcal{D}a = 10^{-5}$ after a) $20L_c$; b) $60L_c$; c) $100L_c$.

For all the different situations, the model provides a very good approximation of the physics at the pore-scale. As previously discussed, the non-equilibrium model is time-constrained because of the hypothesis of quasi-stationarity on $\hat{c}_i$. In this section, we are interested in global stationarity, that is, a special time-constrained situation for which the quasi-stationarity hypothesis is very well satisfied. However, for $\mathcal{P}e = 100$, $\mathcal{D}a = 100$ and $\mathcal{P}e = 1000$, $\mathcal{D}a = 1000$ some discrepancies arise between the different normalizations. If the concentration is normalized using $\langle c\rangle^{\gamma\omega}$ calculated on a cell far away from the input boundary, the results are closer between the DNS and the homogenized model. The reason for this is that, in the DNS, by imposing a Dirichlet boundary input, we impose $\tilde{c}_\gamma = 0$ and this cannot be captured by the macroscopic model. As a consequence, the flux on $\mathcal{S}_{\gamma\omega}$ is overestimated in the DNS on the first cells as compared to the homogenized model. When $\mathcal{P}e = 10$, $\mathcal{D}a = 10$, this overestimation does not even reach the second cell. For $\mathcal{P}e = 100$, $\mathcal{D}a = 100$, it starts to exceed the first cell. For $\mathcal{P}e = 1000$, $\mathcal{D}a = 1000$, the discrepancy propagates very far from the boundary input as even the normalization on the cell number 20 does not give a satisfying result as compared to the one on the cell number 40. These discrepancies appear because of the specific ordering of the porous medium and would not propagate so far from the input in a disordered medium. This question of the impact of boundary conditions on the comparison between direct numerical simulations and macroscopic predictions has received some attention in the literature [64–66]. Corrections of the macroscale boundary conditions, or mixed microscale/macroscale approaches are available [65–67] but this is beyond the scope of this paper to develop such techniques.

5.3.2. Transient analysis

In this subsection, we study the transient behaviors of the one-equation non-equilibrium and equilibrium models for a square input of width $\delta t' = 5$ starting at $t' = 0$. Concentrations are normalized to the amplitude of the square input and the time t' is normalized with the characteristic time associated to the advective term. Notice that in

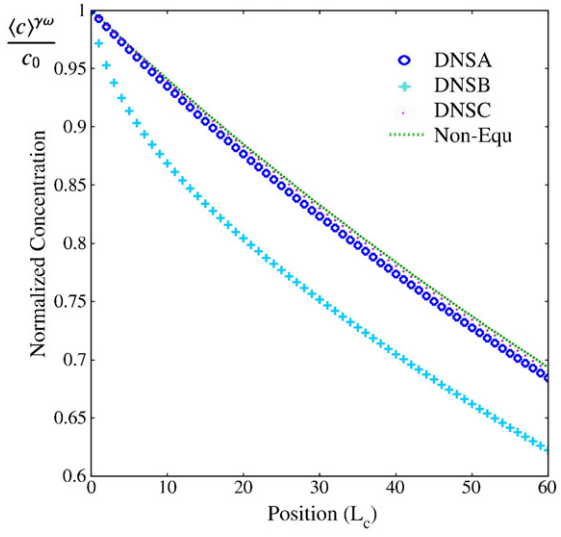

Fig. 12. DNS and non-equilibrium model stationary concentration fields for $\mathcal{P}e = 1000$ and $\mathcal{D}a = 1000$ using normalization on the first cell (DNSB), on the cell number 20 (DNSA) and on the cell number 40 (DNSC).

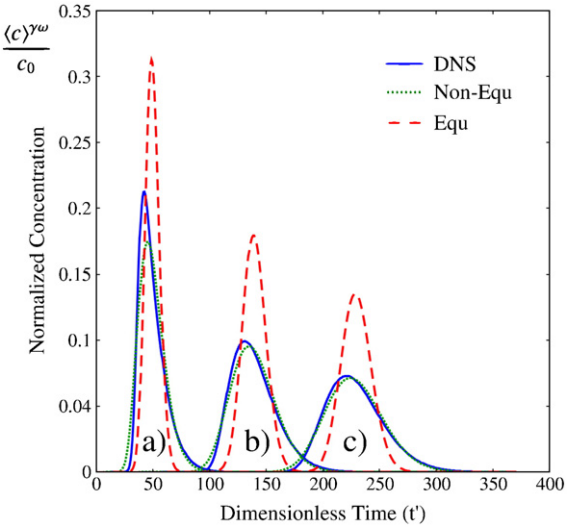

Fig. 14. Transient breakthrough curves for the DNS, the local non-equilibrium and equilibrium models for a square input of $\delta t' = 5$ for $\mathcal{P}e = 100$ and $\mathcal{D}a = 10^{-5}$ after a) $20L_c$; b) $60L_c$; c) $100L_c$.

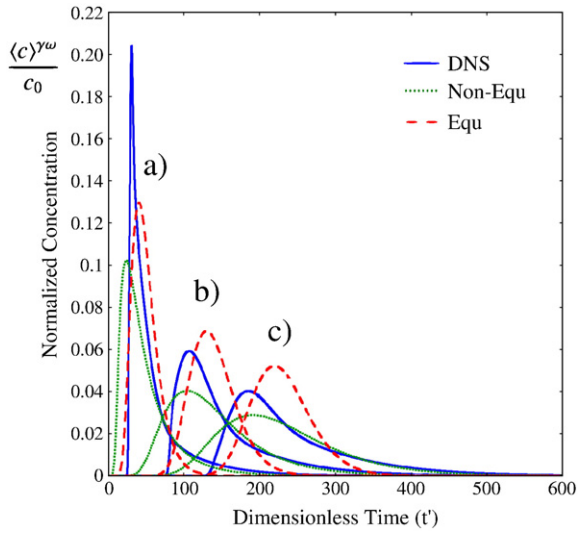

Fig. 15. Transient breakthrough curves for the DNS, the local non-equilibrium and equilibrium models for a square input of $\delta t' = 5$ for $\mathcal{P}e = 1000$ and $\mathcal{D}a = 10^{-5}$ after a) $20L_c$; b) $60L_c$; c) $100L_c$.

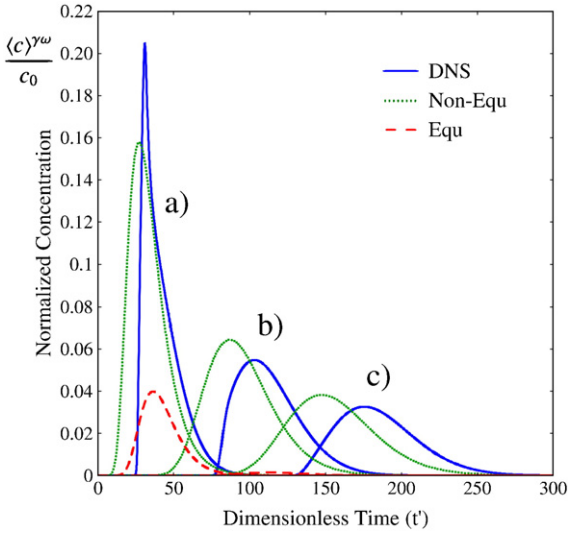

Fig. 17. Transient breakthrough curves for the DNS, the local non-equilibrium and equilibrium models for a square input of $\delta t' = 5$ for $\mathcal{P}e = 1000$ and $\mathcal{D}a = 1000$ after a) $20L_c$; b) $60L_c$; c) $100L_c$.

the transient case, we cannot avoid the issue previously presented as the concentration cannot be renormalized straighforwardly.

5.3.2.1. Influence of the $\mathcal{P}e$ number. On Fig. 13, the three homogenized models provide a very good approximation of the transport problem. At low Péclet, low Damköhler numbers, time and space non-locality tend to disappear because time and length scales are fully separated. The signal even propagates slowly enough for the local mass equilibrium assumption to be valid. Meanwhile, some very little discrepancy, probably due to the flux overestimation discussed in the Section 5.3.1, exists at the peaks.

When the Péclet number reaches values around 100, the local mass equilibrium assumption becomes clearly inappropriate. Fig. 14 shows that the local mass equilibrium model gives a poor approximation of the signal whereas the non-equilibrium one is still in good agreement. The fact that the peaks for $20L_c$ are not in such a good agreement is characteristic of non-locality. Memory functions (convolutions) or two-equation models should be considered in this case.

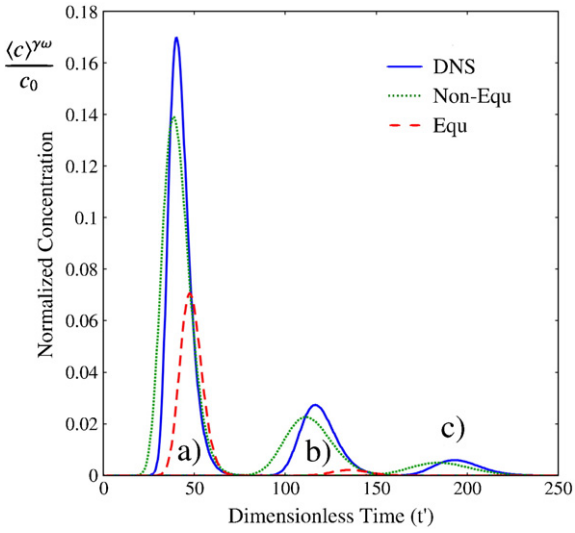

Fig. 16. Transient breakthrough curves for the DNS, the local non-equilibrium and equilibrium models for a square input of $\delta t' = 5$ for $\mathcal{P}e = 100$ and $\mathcal{D}a = 100$ after a) $20L_c$; b) $60L_c$; c) $100L_c$.

However, when the signal spreads, non-locality tends to disappear and the breakthrough curves are in very good agreement.

For Péclet numbers around 1000, Fig. 15, we show that there are some huge discrepancies between both homogenized model and the DNS, especially at $20L_c$ because of the strong non-locality. However, for long times, the non-equilibrium model seems to recover the tailing and the peak of the signal. Results suggest that the one-equation local non-equilibrium model might represent, in cases such as intermediate Péclet numbers or time-asymptotic regime, a good compromise, in terms of computational demand, between fully transient theories and the local mass equilibrium model. The importance of non-locality is also emphasized and becomes particularly obvious in the high Péclet number situation.

5.3.2.2. Influence of the $\mathcal{D}a$ number. When $\mathcal{P}e = 100$ and $\mathcal{D}a = 100$ (Fig. 16) and when $\mathcal{P}e = 1000$ and $\mathcal{D}a = 1000$ (Fig. 17), the local mass equilibrium model obviously does not recover the total mass of the system, that is, the reaction rate is overestimated. The non-equilibrium model is much more correct on this aspect. Meanwhile, at $20L_c$ it fails to capture non-locality and some discrepancies remain even when the signal spreads at $60L_c$ and $100L_c$ unlike for the low $\mathcal{D}a$ situation. This difference probably comes from the overestimation, in the DNS, of the flux on the first cells. In the non-reactive case, this effect has very little influence on the breakthrough curves whereas it is of special importance for high $\mathcal{D}a$ situation as the mass overexchanged disappears. However, unlike the situation $\mathcal{P}e = 1000$ and $\mathcal{D}a = 10^{-5}$, the one-equation non-equilibrium model recovers correctly the shape of the signal. It suggests that in the highly reactive case, the long-time regime may be adhered quicker than in the low reactive case (despite the shift coming from the input boundary discrepancies).

5.4. Conclusions concerning the numerical simulations

First, we study all the effective parameters as functions of $\mathcal{P}e$ and $\mathcal{D}a$ numbers. We show that the dispersion exhibits differences between the reactive and the non-reactive case and this is coherent with other studies [40,62,63]. Effective reaction rate and velocities are also presented and we show that they mainly depend upon the $\mathcal{D}a$ number. We also emphasize that the non-equilibrium model includes the local mass equilibrium one when the conditions of validity of this model are satisfied. From a theoretical point of view, one should

realize that for this special case, the quasi-stationary analysis is the same for both the Gray decomposition and the non-zero averaged decomposition since the local mass equilibrium assumption means $\tilde{c}_\gamma = \hat{c}_\gamma$ and $\tilde{c}_\omega = \hat{c}_\omega$.

Then, by comparison with direct numerical simulations at the pore-scale, we show that the model is perfectly adapted to stationary analysis since this represents a special time-constrained case for which the quasi-stationarity on $\hat{c}_i$ is very well satisfied. We also establish the following limitations

- The model fails to capture very small time phenomena. Two-equation models or fully transient theories may be required in this case. The underlying consequence is that domains of validity for the different models must need a time dimension and not only dimensionless parameters such as $\mathcal{P}e$ and $\mathcal{D}a$ numbers.
- We emphasize that important discrepancies, coming from the boundary conditions, can propagate through the entire system for high $\mathcal{P}e$ and high $\mathcal{D}a$ numbers. Although, it might not propagate so far in disordered media, it requires further investigation.

There are two additional constraints which require supplementary theoretical and numerical research. The first one concerns the assumption on the reaction rate. Herein, we suppose that the concentration of the solute is relatively small, that is, we can consider only linear kinetics. Upscaling of non-linear Monod type reaction rate in a general framework is an area of active research. The second one deals with the assumption that the effective parameters can be calculated on a REV in which the geometry of the biofilm is fixed. For example, in a real medium, one may have to consider fluctuations of the porosities or variations of the representative geometry and it is unclear how these would affect the domain of validity of the time-asymptotic model.

6. Discussion and conclusions

6.1. Relation to other works

In this article, we derive a one-equation non-equilibrium model for solute transport in saturated and biologically reactive porous media. Undertaking the description of multiphase reactive transport using a single one equation approximation has been done countless times by experimenters. However, very few works have focused on developing a theoretical basis and on addressing the validity of this approach. Two situations allowing such a description have been identified in the past and are clarified in our study. On the one hand, when gradients within the bulk phases are relatively small, a single partial differential equation on the concentration in the water-phase can be used to describe the mass transport. This situation is often referred to as the local mass equilibrium condition and has been extensively discussed in [24,26]. On the other hand, it has been suggested that a completely different type of constraint can be formulated to allow a description with merely one equation. Cunningham and Mendoza-Sanchez in [21] have shown that the one-equation model is strictly equivalent to the multicontinuum approach under steady state conditions. This behavior has also been proved many years before in the non-reactive case by Zanotti and Carbonell in [39].

Our analysis can be seen as an extension and a complement of the works by Cunningham and Mendoza-Sanchez [21] and by Dykaar and Kitanidis [40]. In comparison with the work by Cunningham and Mendoza-Sanchez, we provide a direct connection between the microscopic processes and the macroscale description for, virtually, extremely complex topologies. Our development is based on the calculation of the effective parameters on a representative volume possibly accounting for very complex geometries. In addition to the approach by Dykaar and Kitanidis, we propose to take into account the total mass in the system rather than just the mass in the water-phase. The strategy adopted in [40] is clearly an extension of the work by Shapiro and Brenner [63] but additional constraints are necessary in the multiphase situation and this is not clearly emphasized. The domain of validity of our model is clearly established on the basis of (1) comparisons between the upscaled results and the direct numerical simulations at the pore-scale and (2) discussions concerning the first-order closure and the quasi-stationarity of the problems on the perturbations.

Concerning the technique itself, we use a $\hat{c}$ decomposition for concentrations which is a more general case of the one introduced in [45] for mass transport and in [68] for heat transfer. We start our analysis with the microscale description of the medium and then average the equations to obtain a Darcy-scale description of the medium. In short times, the multidomain approach provides a better approximation of the transport processes because, the closure on the $\tilde{c}$ fluctuations captures more characteristic times and because, as previously discussed, the quasi-stationarity of the perturbation problem on $\hat{c}$ is much stronger than the one on $\tilde{c}$. In the non-reactive situation, these theoretical aspects have been extensively described in [39] and in [41] but this is the first application to a reactive situation.

6.2. General conclusions

In past research, the calculation of effective parameters has been largely undertaken using tracer techniques and inverse optimization on the basis of empirical models. The main problems with this approach are that (1) the macroscale equation are elaborated on the basis of simple conceptual schemes and it is unclear how much information these models are able to capture, (2) the effective parameters, say the dispersion, are often considered as intrinsic to a medium and not recalculated every time a physical parameter such as the Péclet number is modified and (3) there is no clear relationship between the definition of the macroscopic concentrations and the concentration measured.

Given the advances in terms of imaging techniques [60,61] and of understanding of the transport processes, we believe that upscaling represents an alternative in many cases. The volume averaging theory lends itself very well for the exploration of the physics of the transport as well as for the expression of the effective parameters as a function of the microscale processes on a representative volume.

In conclusion, we provide a solid theoretical background for the one-equation model along with (1) constraints concerning its validity, (2) a method for the calculation of the effective parameters and (3) a precise definition of the macroscopic concentration. When applying the model to experimental results, these three points should be carefully examined.

Acknowledgements

Support from CNRS/GdR 2990 is gratefully acknowledged. The third author (BDW) was supported in part by the Office of Science (BER), U.S. Department of Energy, Grant No. DE-FG02-07ER64417.

Appendix A

In this Appendix, we develop the volume averaged equations for each phase. We start with the pore-scale description of the medium

$$\gamma\text{–phase}: \quad \frac{\partial c_\gamma}{\partial t} + \nabla\cdot\left(c_\gamma \mathbf{v}_\gamma\right) = \nabla\cdot\left(\mathbf{D}_\gamma\cdot\nabla c_\gamma\right) \tag{85}$$

$$BC1: \quad -\left(\mathbf{n}_{\gamma\sigma}\cdot\mathbf{D}_\gamma\right)\cdot\nabla c_\gamma = 0 \qquad \text{on } \mathcal{S}_{\gamma\sigma} \tag{86a}$$

$$BC2: \quad c_\omega = c_\gamma \qquad \text{on } \mathcal{S}_{\gamma\omega} \tag{86b}$$

$$BC3: \quad -\left(\mathbf{n}_{\gamma\omega}\cdot\mathbf{D}_{\gamma}\right)\cdot\nabla c_{\gamma} = -\left(\mathbf{n}_{\gamma\omega}\cdot\mathbf{D}_{\omega}\right)\cdot\nabla c_{\omega} \qquad \text{on } \mathcal{S}_{\gamma\omega} \tag{86c}$$

$$BC4: \quad \left(\mathbf{n}_{\omega\sigma}\cdot\mathbf{D}_{\omega}\right)\cdot\nabla c_{\omega} = 0 \qquad \text{on } \mathcal{S}_{\omega\sigma} \tag{86d}$$

$$\omega-\text{phase}: \quad \frac{\partial c_{\omega}}{\partial t} = \nabla\cdot\left(\mathbf{D}_{\omega}\cdot\nabla c_{\omega}\right) + \mathcal{R}_{\omega}. \tag{87}$$

To develop equations governing mass transport at the macroscopic scale, we need to average each equation

$$\gamma-\text{phase}: \quad \left\langle\frac{\partial c_{\gamma}}{\partial t}\right\rangle + \left\langle\nabla\cdot\left(c_{\gamma}\mathbf{v}_{\gamma}\right)\right\rangle = \left\langle\nabla\cdot\left(\mathbf{D}_{\gamma}\cdot\nabla c_{\gamma}\right)\right\rangle \tag{88}$$

$$\omega-\text{phase}: \quad \left\langle\frac{\partial c_{\omega}}{\partial t}\right\rangle = \langle\nabla\cdot\left(\mathbf{D}_{\omega}\cdot\nabla c_{\omega}\right)\rangle + \langle\mathcal{R}_{\omega}\rangle. \tag{89}$$

Then, we are confronted to the classical problem of averaging time derivatives and spatial operators. For this purpose, we use the following theorems

General transport theorem [69]

$$\left\langle\frac{\partial c_{\gamma}}{\partial t}\right\rangle = \frac{\partial\left\langle c_{\gamma}\right\rangle}{\partial t} - \frac{1}{V}\int_{\mathcal{S}_{\gamma\omega}(t)}\left(\mathbf{n}_{\gamma\omega}\cdot\mathbf{w}\right)c_{\gamma}dS \tag{90}$$

$$\left\langle\frac{\partial c_{\omega}}{\partial t}\right\rangle = \frac{\partial\langle c_{\omega}\rangle}{\partial t} - \frac{1}{V}\int_{\mathcal{S}_{\omega\gamma}(t)}\left(\mathbf{n}_{\omega\gamma}\cdot\mathbf{w}\right)c_{\omega}dS \tag{91}$$

with $\mathbf{w}$ the velocity of the interface.

Spatial averaging theorems [70,71]

$$\left\langle\nabla c_{\gamma}\right\rangle = \nabla\left\langle c_{\gamma}\right\rangle + \frac{1}{V}\int_{\mathcal{S}_{\gamma\omega}}\mathbf{n}_{\gamma\omega}c_{\gamma}dS + \frac{1}{V}\int_{\mathcal{S}_{\gamma\sigma}}\mathbf{n}_{\gamma\sigma}c_{\gamma}dS \tag{92}$$

$$\langle\nabla c_{\omega}\rangle = \nabla\langle c_{\omega}\rangle + \frac{1}{V}\int_{\mathcal{S}_{\omega\gamma}}\mathbf{n}_{\omega\gamma}c_{\omega}dS + \frac{1}{V}\int_{\mathcal{S}_{\omega\sigma}}\mathbf{n}_{\omega\sigma}c_{\omega}dS. \tag{93}$$

Hence, we have

$$\begin{aligned}\gamma-\text{phase}: &\frac{\partial\varepsilon_{\gamma}\left\langle c_{\gamma}\right\rangle^{\gamma}}{\partial t} - \frac{1}{V}\int_{\mathcal{S}_{\gamma\omega}(t)}\left(\mathbf{n}_{\gamma\omega}\cdot\mathbf{w}\right)c_{\gamma}dS + \nabla\cdot\left(\varepsilon_{\gamma}\langle c\rangle^{\gamma\omega}\left\langle\mathbf{v}_{\gamma}\right\rangle^{\gamma}\right) \\ &= \nabla\cdot\left\{\mathbf{D}_{\gamma}\cdot\nabla\left(\varepsilon_{\gamma}\left\langle c_{\gamma}\right\rangle^{\gamma}\right)\right\} + \nabla\cdot\left\{\mathbf{D}_{\gamma}\cdot\left(\frac{1}{V}\int_{\mathcal{S}_{\gamma\omega}}\mathbf{n}_{\gamma\omega}c_{\gamma}dS + \frac{1}{V}\int_{\mathcal{S}_{\gamma\sigma}}\mathbf{n}_{\gamma\sigma}c_{\gamma}dS\right)\right\} \\ &+ \frac{1}{V}\int_{\mathcal{S}_{\gamma\omega}}\left(\mathbf{n}_{\gamma\omega}\cdot\mathbf{D}_{\gamma}\right)\cdot\nabla c_{\gamma}dS + \frac{1}{V}\int_{\mathcal{S}_{\gamma\sigma}}\left(\mathbf{n}_{\gamma\sigma}\cdot\mathrm{D}_{\gamma}\right)\cdot\nabla c_{\gamma}dS - \nabla\cdot\left\langle\hat{c}_{\gamma}\mathbf{v}_{\gamma}\right\rangle\end{aligned} \tag{94}$$

$$\begin{aligned}\omega-\text{phase}: &\frac{\partial\varepsilon_{\omega}\langle c_{\omega}\rangle^{\omega}}{\partial t} - \frac{1}{V}\int_{\mathcal{S}_{\omega\gamma}(t)}\left(\mathbf{n}_{\omega\gamma}\cdot\mathbf{w}\right)c_{\omega} \\ &= \nabla\cdot\left\{\mathbf{D}_{\omega}\cdot\left(\nabla\{\varepsilon_{\omega}\langle c_{\omega}\rangle^{\omega}\} + \frac{1}{V}\int_{\mathcal{S}_{\omega\gamma}}\mathbf{n}_{\omega\gamma}c_{\omega}dS + \frac{1}{V}\int_{\mathcal{S}_{\omega\sigma}}\mathbf{n}_{\omega\sigma}c_{\omega}dS\right)\right\} \\ &+ \frac{1}{V}\int_{\mathcal{S}_{\omega\gamma}}\left(\mathbf{n}_{\omega\gamma}\cdot\mathbf{D}_{\omega}\right)\cdot\nabla c_{\omega}dS + \frac{1}{V}\int_{\mathcal{S}_{\omega\sigma}}\left(\mathbf{n}_{\omega\sigma}\cdot\mathbf{D}_{\omega}\right)\cdot\nabla c_{\omega}dS + \varepsilon_{\omega}\langle\mathcal{R}_{\omega}\rangle^{\omega}.\end{aligned} \tag{95}$$

It has already been emphasized [17] that characteristic times associated to biofilm motion are long as compared to the one associated with the mass transport so that we can write

$$\begin{aligned}\gamma-\text{phase}: &\frac{\partial\varepsilon_{\gamma}\left\langle c_{\gamma}\right\rangle^{\gamma}}{\partial t} + \nabla\cdot\left(\varepsilon_{\gamma}\langle c\rangle^{\gamma\omega}\left\langle\mathbf{v}_{\gamma}\right\rangle^{\gamma}\right) \\ &= \nabla\cdot\left\{\mathbf{D}_{\gamma}\cdot\left(\nabla\left\{\varepsilon_{\gamma}\left\langle c_{\gamma}\right\rangle^{\gamma}\right\} + \frac{1}{V}\int_{\mathcal{S}_{\gamma\omega}}\mathbf{n}_{\gamma\omega}c_{\gamma}dS + \frac{1}{V}\int_{\mathcal{S}_{\gamma\sigma}}\mathbf{n}_{\gamma\sigma}c_{\gamma}dS\right)\right\} \\ &+ \frac{1}{V}\int_{\mathcal{S}_{\gamma\omega}}\left(\mathbf{n}_{\gamma\omega}\cdot\mathbf{D}_{\gamma}\right)\cdot\nabla c_{\gamma}dS + \frac{1}{V}\int_{\mathcal{S}_{\gamma\sigma}}\left(\mathbf{n}_{\gamma\sigma}\cdot\mathbf{D}_{\gamma}\right)\cdot\nabla c_{\gamma}dS - \nabla\cdot\left\langle\hat{c}_{\gamma}\mathbf{v}_{\gamma}\right\rangle\end{aligned} \tag{96}$$

$$\begin{aligned}\omega-\text{phase}: &\frac{\partial\varepsilon_{\omega}\langle c_{\omega}\rangle^{\omega}}{\partial t} = \nabla\cdot\left\{\mathbf{D}_{\omega}\cdot\left(\nabla\{\varepsilon_{\omega}\langle c_{\omega}\rangle^{\omega}\} + \frac{1}{V}\int_{\mathcal{S}_{\omega\gamma}}\mathbf{n}_{\omega\gamma}c_{\omega}dS + \frac{1}{V}\int_{\mathcal{S}_{\omega\sigma}}\mathbf{n}_{\omega\sigma}c_{\omega}dS\right)\right\} \\ &+ \frac{1}{V}\int_{\mathcal{S}_{\omega\gamma}}\left(\mathbf{n}_{\omega\gamma}\cdot\mathbf{D}_{\omega}\right)\cdot\nabla c_{\omega}dS + \frac{1}{V}\int_{\mathcal{S}_{\omega\sigma}}\left(\mathbf{n}_{\omega\sigma}\cdot\mathbf{D}_{\omega}\right)\cdot\nabla c_{\omega}dS \\ &+ \varepsilon_{\omega}\langle\mathcal{R}_{\omega}\rangle^{\omega}.\end{aligned} \tag{97}$$

We use the following decompositions $c_{\gamma} = \langle c_{\gamma}\rangle^{\gamma} + \tilde{c}_{\gamma}$, $c_{\omega} = \langle c_{\omega}\rangle^{\omega} + \tilde{c}_{\omega}$ and

$$\langle c_{\omega}\rangle^{\omega}_{\mathbf{x}+\mathbf{y}} = \langle c_{\omega}\rangle^{\omega}_{\mathbf{x}} + \mathbf{y}\cdot\nabla\langle c_{\omega}\rangle^{\omega}_{\mathbf{x}} + \cdots \tag{98}$$

$$\left\langle c_{\gamma}\right\rangle^{\gamma}_{\mathbf{x}+\mathbf{y}} = \left\langle c_{\gamma}\right\rangle^{\gamma}_{\mathbf{x}} + \mathbf{y}\cdot\nabla\left\langle c_{\gamma}\right\rangle^{\gamma}_{\mathbf{x}} + \cdots \tag{99}$$

where $\mathbf{x}$ is the vector pointing the position of the center of the REV and $\mathbf{y}$ is the vector pointing inside the REV. Then we can neglect all the non-local terms involving y provided that $R_0^2 \ll L^2$ [27], where L is a characteristic field-scale length, and this is expressed by

$$\begin{aligned}&\frac{1}{V}\int_{\mathcal{S}_{\gamma\omega}}\mathbf{n}_{\gamma\omega}c_{\gamma}dS + \frac{1}{V}\int_{\mathcal{S}_{\gamma\sigma}}\mathbf{n}_{\gamma\sigma}c_{\gamma}dS \\ &= \frac{1}{V}\int_{\mathcal{S}_{\gamma\omega}}\mathbf{n}_{\gamma\omega}\left\langle c_{\gamma}\right\rangle^{\gamma}_{\mathbf{x}+\mathbf{y}}dS + \frac{1}{V}\int_{\mathcal{S}_{\gamma\sigma}}\mathbf{n}_{\gamma\sigma}\left\langle c_{\gamma}\right\rangle^{\gamma}_{\mathbf{x}+\mathbf{y}}dS \\ &\quad + \frac{1}{V}\int_{\mathcal{S}_{\gamma\omega}}\mathbf{n}_{\gamma\omega}\tilde{c}_{\gamma}dS + \frac{1}{V}\int_{\mathcal{S}_{\gamma\sigma}}\mathbf{n}_{\gamma\sigma}\tilde{c}_{\gamma}dS \\ &\simeq\left\langle c_{\gamma}\right\rangle^{\gamma}_{\mathbf{x}}\left(\frac{1}{V}\int_{\mathcal{S}_{\gamma\omega}}\mathbf{n}_{\gamma\omega}dS + \frac{1}{V}\int_{\mathcal{S}_{\gamma\sigma}}\mathbf{n}_{\sigma\omega}dS\right) \\ &\quad + \frac{1}{V}\int_{\mathcal{S}_{\gamma\omega}}\mathbf{n}_{\gamma\omega}\tilde{c}_{\gamma}dS + \frac{1}{V}\int_{\mathcal{S}_{\gamma\sigma}}\mathbf{n}_{\gamma\sigma}\tilde{c}_{\gamma}dS\end{aligned} \tag{100}$$

$$\begin{aligned}&\frac{1}{V}\int_{\mathcal{S}_{\omega\gamma}}\mathbf{n}_{\omega\gamma}c_{\omega}dS + \frac{1}{V}\int_{\mathcal{S}_{\omega\sigma}}\mathbf{n}_{\omega\sigma}c_{\omega}dS \\ &= \frac{1}{V}\int_{\mathcal{S}_{\omega\gamma}}\mathbf{n}_{\omega\gamma}\langle c_{\omega}\rangle^{\omega}_{\mathbf{x}+\mathbf{y}}dS + \frac{1}{V}\int_{\mathcal{S}_{\omega\sigma}}\mathbf{n}_{\omega\sigma}\langle c_{\omega}\rangle^{\omega}_{\mathbf{x}+\mathbf{y}}dS \\ &\quad + \frac{1}{V}\int_{\mathcal{S}_{\omega\gamma}}\mathbf{n}_{\omega\gamma}\tilde{c}_{\omega}dS + \frac{1}{V}\int_{\mathcal{S}_{\omega\sigma}}\mathbf{n}_{\omega\sigma}\tilde{c}_{\omega}dS \\ &\simeq\langle c_{\omega}\rangle^{\omega}_{\mathbf{x}}\left(\frac{1}{V}\int_{\mathcal{S}_{\omega\gamma}}\mathbf{n}_{\omega\gamma}dS + \frac{1}{V}\int_{\mathcal{S}_{\omega\sigma}}\mathbf{n}_{\omega\sigma}dS\right) \\ &\quad + \frac{1}{V}\int_{\mathcal{S}_{\omega\gamma}}\mathbf{n}_{\omega\gamma}\tilde{c}_{\omega}dS + \frac{1}{V}\int_{\mathcal{S}_{\omega\sigma}}\mathbf{n}_{\omega\sigma}\tilde{c}_{\omega}dS.\end{aligned} \tag{101}$$

Then, using spatial averaging theorems for unity gives

$$-\nabla\varepsilon_{\omega} = \frac{1}{V}\int_{\mathcal{S}_{\omega\gamma}}\mathbf{n}_{\omega\gamma}dS + \frac{1}{V}\int_{\mathcal{S}_{\omega\sigma}}\mathbf{n}_{\omega\sigma}dS \tag{102}$$

$$-\nabla\varepsilon_{\gamma} = \frac{1}{V}\int_{\mathcal{S}_{\gamma\omega}}\mathbf{n}_{\gamma\omega}dS + \frac{1}{V}\int_{\mathcal{S}_{\gamma\sigma}}\mathbf{n}_{\gamma\sigma}dS. \tag{103}$$

Hence, we have

$$\begin{aligned}&\frac{1}{V}\int_{\mathcal{S}_{\omega\gamma}}\mathbf{n}_{\omega\gamma}c_{\omega}dS + \frac{1}{V}\int_{\mathcal{S}_{\omega\sigma}}\mathbf{n}_{\omega\sigma}c_{\omega}dS \\ &\simeq -\nabla\varepsilon_{\omega}\langle c_{\omega}\rangle^{\omega}_{\mathbf{x}} + \frac{1}{V}\int_{\mathcal{S}_{\omega\gamma}}\mathbf{n}_{\omega\gamma}\tilde{c}_{\omega}dS + \frac{1}{V}\int_{\mathcal{S}_{\omega\sigma}}\mathbf{n}_{\omega\sigma}\tilde{c}_{\omega}dS\end{aligned} \tag{104}$$

$$\begin{aligned}&\frac{1}{V}\int_{\mathcal{S}_{\gamma\omega}}\mathbf{n}_{\gamma\omega}c_{\gamma}dS + \frac{1}{V}\int_{\mathcal{S}_{\gamma\sigma}}\mathbf{n}_{\gamma\sigma}c_{\gamma}dS \\ &\simeq -\nabla\varepsilon_{\gamma}\left\langle c_{\gamma}\right\rangle^{\gamma}_{\mathbf{x}} + \frac{1}{V}\int_{\mathcal{S}_{\gamma\omega}}\mathbf{n}_{\gamma\omega}\tilde{c}_{\gamma}dS + \frac{1}{V}\int_{\mathcal{S}_{\gamma\sigma}}\mathbf{n}_{\sigma\omega}\tilde{c}_{\gamma}dS.\end{aligned} \tag{105}$$

Finally, injecting Eqs. (104) and (105) into Eqs. (94) and (95) leads to

$$\gamma\text{–phase}: \frac{\partial \varepsilon_\gamma \left\langle c_\gamma \right\rangle^\gamma}{\partial t} + \nabla\cdot\left(\varepsilon_\gamma \langle c\rangle^{\gamma\omega}\left\langle \mathbf{v}_\gamma \right\rangle^\gamma\right) = \nabla\cdot\left\{\varepsilon_\gamma \mathbf{D}_\gamma\cdot\ \nabla\left\langle c_\gamma\right\rangle^\gamma + \frac{1}{V_\gamma}\int_{S_{\gamma\omega}} \mathbf{n}_{\gamma\omega}\tilde{c}_\gamma dS + \frac{1}{V_\gamma}\int_{S_{\gamma\sigma}} \mathbf{n}_{\gamma\sigma}\tilde{c}_\gamma dS\right)\right\} + \frac{1}{V}\int_{S_{\gamma\omega}} (\mathbf{n}_{\gamma\omega}\cdot\mathbf{D}_\gamma)\cdot\nabla c_\gamma dS + \frac{1}{V}\int_{S_{\gamma\sigma}} (\mathbf{n}_{\gamma\sigma}\cdot\mathbf{D}_\gamma)\cdot\nabla c_\gamma dS - \nabla\cdot\left\langle \hat{c}_\gamma \mathbf{v}_\gamma\right\rangle \tag{106}$$

$$\omega\text{–phase}: \frac{\partial \varepsilon_\omega \langle c_\omega\rangle^\omega}{\partial t} = \nabla\cdot\left\{\varepsilon_\omega \mathbf{D}_\omega\cdot\left(\nabla\langle c_\omega\rangle^\omega + \frac{1}{V_\omega}\int_{S_{\omega\gamma}} \mathbf{n}_{\omega\gamma}\tilde{c}_\omega dS + \frac{1}{V_\omega}\int_{S_{\omega\sigma}} \mathbf{n}_{\omega\sigma}\tilde{c}_\omega dS\right)\right\} + \frac{1}{V}\int_{S_{\omega\gamma}} (\mathbf{n}_{\omega\gamma}\cdot\mathbf{D}_\omega)\cdot\nabla c_\omega dS + \frac{1}{V}\int_{S_{\omega\sigma}} (\mathbf{n}_{\omega\sigma}\cdot\mathbf{D}_\omega)\cdot\nabla c_\omega dS + \varepsilon_\omega\langle\mathcal{R}_\omega\rangle^\omega. \tag{107}$$

Appendix B

In this part, we develop the macroscopic one-equation non-closed form of the model starting with the averaged equations for each phase

$$\gamma\text{–phase}: \frac{\partial \varepsilon_\gamma \left\langle c_\gamma \right\rangle^\gamma}{\partial t} + \nabla\cdot\left(\varepsilon_\gamma \langle c\rangle^{\gamma\omega}\left\langle \mathbf{v}_\gamma \right\rangle^\gamma\right) = \nabla\cdot\left\{\varepsilon_\gamma \mathbf{D}_\gamma\cdot\ \nabla\left\langle c_\gamma\right\rangle^\gamma + \frac{1}{V_\gamma}\int_{S_{\gamma\omega}} \mathbf{n}_{\gamma\omega}\tilde{c}_\gamma dS + \frac{1}{V_\gamma}\int_{S_{\gamma\sigma}} \mathbf{n}_{\gamma\sigma}\tilde{c}_\gamma dS\right)\right\} + \frac{1}{V}\int_{S_{\gamma\omega}} (\mathbf{n}_{\gamma\omega}\cdot\mathbf{D}_\gamma)\cdot\nabla c_\gamma dS + \frac{1}{V}\int_{S_{\gamma\sigma}} (\mathbf{n}_{\gamma\sigma}\cdot\mathbf{D}_\gamma)\cdot\nabla c_\gamma dS - \nabla\cdot\left\langle \hat{c}_\gamma \mathbf{v}_\gamma\right\rangle \tag{108}$$

$$\omega\text{–phase}: \frac{\partial \varepsilon_\omega \langle c_\omega\rangle^\omega}{\partial t} = \nabla\cdot\left\{\varepsilon_\omega \mathbf{D}_\omega\cdot\left(\nabla\langle c_\omega\rangle^\omega + \frac{1}{V_\omega}\int_{S_{\omega\gamma}} \mathbf{n}_{\omega\gamma}\tilde{c}_\omega dS + \frac{1}{V_\omega}\int_{S_{\omega\sigma}} \mathbf{n}_{\omega\sigma}\tilde{c}_\omega dS\right)\right\} + \frac{1}{V}\int_{S_{\omega\gamma}} (\mathbf{n}_{\omega\gamma}\cdot\mathbf{D}_\omega)\cdot\nabla c_\omega dS + \frac{1}{V}\int_{S_{\omega\sigma}} (\mathbf{n}_{\omega\sigma}\cdot\mathbf{D}_\omega)\cdot\nabla c_\omega dS + \varepsilon_\omega\langle\mathcal{R}_\omega\rangle^\omega. \tag{109}$$

Then, we make the flux term disappear by summing equations over the γ-phase and the ω-phase and by using the flux-continuity hypothesis at the interface between γ and ω.

$$\frac{\partial\langle c\rangle}{\partial t} + \nabla\cdot\left(\varepsilon_\gamma\langle c\rangle^{\gamma\omega}\left\langle \mathbf{v}_\gamma\right\rangle^\gamma\right) = \nabla\cdot\left\{\varepsilon_\omega \mathbf{D}_\omega\cdot\nabla\langle c_\omega\rangle^\omega + \varepsilon_\gamma \mathbf{D}_\gamma\cdot\nabla\left\langle c_\gamma\right\rangle^\gamma\right\} + \nabla\cdot\left\{\mathbf{D}_\omega\cdot\left(\frac{1}{V}\int_{S_{\omega\gamma}} \mathbf{n}_{\omega\gamma}\tilde{c}_\omega dS + \frac{1}{V}\int_{S_{\omega\sigma}} \mathbf{n}_{\omega\sigma}\tilde{c}_\omega dS\right)\right\} + \nabla\cdot\left\{\mathbf{D}_\gamma\cdot\left(\frac{1}{V}\int_{S_{\gamma\omega}} \mathbf{n}_{\gamma\omega}\tilde{c}_\gamma dS + \frac{1}{V}\int_{S_{\gamma\sigma}} \mathbf{n}_{\gamma\sigma}\tilde{c}_\gamma dS\right)\right\} + \varepsilon_\omega\langle\mathcal{R}_\omega\rangle^\omega - \nabla\cdot\left\langle\hat{c}_\gamma\mathbf{v}_\gamma\right\rangle. \tag{110}$$

Then, we make intrinsic total average equation appear dividing by $\varepsilon_\gamma+\varepsilon_\omega$ (supposed constant over time and space) as it is the one used in the decompositions of concentrations.

$$\frac{\partial\langle c\rangle^{\gamma\omega}}{\partial t} + \nabla\cdot\ \frac{\varepsilon_\gamma}{\varepsilon_\gamma+\varepsilon_\omega}\langle c\rangle^{\gamma\omega}\left\langle\mathbf{v}_\gamma\right\rangle^\gamma\Big) = \nabla\cdot\left\{\frac{\varepsilon_\omega}{\varepsilon_\gamma+\varepsilon_\omega}\mathbf{D}_\omega\cdot\nabla\langle c_\omega\rangle^\omega + \frac{\varepsilon_\gamma}{\varepsilon_\gamma+\varepsilon_\omega}\mathbf{D}_\gamma\cdot\nabla\left\langle c_\gamma\right\rangle^\gamma\right\} + \nabla\cdot\left\{\frac{\varepsilon_\omega}{\varepsilon_\gamma+\varepsilon_\omega}\mathbf{D}_\omega\cdot\left(\frac{1}{V_\omega}\int_{S_{\omega\gamma}}\mathbf{n}_{\omega\gamma}\hat{c}_\omega dS + \frac{1}{V\omega}\int_{S_{\omega\sigma}}\mathbf{n}_{\omega\sigma}\hat{c}_\omega dS\right)\right\} + \nabla\cdot\left\{\frac{\varepsilon_\gamma}{\varepsilon_\gamma+\varepsilon_\omega}\mathbf{D}_\gamma\cdot\ \frac{1}{V_\gamma}\int_{S_{\gamma\omega}}\mathbf{n}_{\gamma\omega}\hat{c}_\gamma dS + \frac{1}{V_\gamma}\int_{S_{\gamma\sigma}}\mathbf{n}_{\gamma\sigma}\hat{c}_\gamma dS\right)\right\} + \frac{\varepsilon_\omega}{\varepsilon_\gamma+\varepsilon_\omega}\langle\mathcal{R}_\omega\rangle^\omega - \frac{1}{\varepsilon_\gamma+\varepsilon_\omega}\nabla\cdot\left\langle\hat{c}_\gamma\mathbf{v}_\gamma\right\rangle. \tag{111}$$

Finally, we use the following relations

$$\left\langle c_\gamma\right\rangle^\gamma = \langle c\rangle^{\gamma\omega} + \left\langle\hat{c}_\gamma\right\rangle^\gamma \tag{112}$$

$$\langle c_\omega\rangle^\omega = \langle c\rangle^{\gamma\omega} + \langle\hat{c}_\omega\rangle^\omega \tag{113}$$

$$\tilde{c}_\gamma = \hat{c}_\gamma - \left\langle\hat{c}_\gamma\right\rangle^\gamma \tag{114}$$

$$\tilde{c}_\omega = \hat{c}_\omega - \langle\hat{c}_\omega\rangle^\omega \tag{115}$$

which gives

$$\frac{\partial\langle c\rangle^{\gamma\omega}}{\partial t} + \nabla\cdot\ \frac{\varepsilon_\gamma}{\varepsilon_\gamma+\varepsilon_\omega}\langle c\rangle^{\gamma\omega}\left\langle\mathbf{v}_\gamma\right\rangle^\gamma\Big) = \nabla\cdot\left\{\ \frac{\varepsilon_\omega}{\varepsilon_\gamma+\varepsilon_\omega}\mathbf{D}_\omega + \frac{\varepsilon_\gamma}{\varepsilon_\gamma+\varepsilon_\omega}\mathbf{D}_\gamma\right)\cdot\nabla\langle c\rangle^{\gamma\omega}\right\} + \nabla\cdot\left\{\frac{\varepsilon_\omega}{\varepsilon_\gamma+\varepsilon_\omega}\mathbf{D}_\omega\cdot\nabla\langle\hat{c}_\omega\rangle^\omega + \frac{\varepsilon_\gamma}{\varepsilon_\gamma+\varepsilon_\omega}\mathbf{D}_\gamma\cdot\nabla\left\langle\hat{c}_\gamma\right\rangle^\gamma\right\} + \nabla\cdot\left\{\frac{\varepsilon_\omega}{\varepsilon_\gamma+\varepsilon_\omega}\mathbf{D}_\omega\cdot\left(\frac{1}{V_\omega}\int_{S_{\omega\gamma}}\mathbf{n}_{\omega\gamma}\hat{c}_\omega dS + \frac{1}{V_\omega}\int_{S_{\omega\sigma}}\mathbf{n}_{\omega\sigma}\hat{c}_\omega dS\right)\right\} + \nabla\cdot\left\{\frac{\varepsilon_\gamma}{\varepsilon_\gamma+\varepsilon_\omega}\mathbf{D}_\gamma\cdot\ \frac{1}{V_\gamma}\int_{S_{\gamma\omega}}\mathbf{n}_{\gamma\omega}\hat{c}_\gamma dS + \frac{1}{V_\gamma}\int_{S_{\gamma\sigma}}\mathbf{n}_{\gamma\sigma}\hat{c}_\gamma dS\right)\right\} - \nabla\cdot\left\{\frac{\varepsilon_\omega}{\varepsilon_\gamma+\varepsilon_\omega}\mathbf{D}_\omega\cdot\left(\frac{1}{V_\omega}\int_{S_{\omega\gamma}}\mathbf{n}_{\omega\gamma}\langle\hat{c}_\omega\rangle^\omega dS + \frac{1}{V_\omega}\int_{S_{\omega\sigma}}\mathbf{n}_{\omega\sigma}\langle\hat{c}_\omega\rangle^\omega dS\right)\right\} - \nabla\cdot\left\{\frac{\varepsilon_\gamma}{\varepsilon_\gamma+\varepsilon_\omega}\mathbf{D}_\gamma\cdot\ \frac{1}{V_\gamma}\int_{S_{\gamma\omega}}\mathbf{n}_{\gamma\omega}\left\langle\hat{c}_\gamma\right\rangle^\gamma dS + \frac{1}{V_\gamma}\int_{S_{\gamma\sigma}}\mathbf{n}_{\gamma\sigma}\left\langle\hat{c}_\gamma\right\rangle^\gamma dS\right)\right\} + \frac{\varepsilon_\omega}{\varepsilon_\gamma+\varepsilon_\omega}\langle\mathcal{R}_\omega\rangle^\omega - \frac{1}{\varepsilon_\gamma+\varepsilon_\omega}\nabla\cdot\left\langle\hat{c}_\gamma\mathbf{v}_\gamma\right\rangle. \tag{116}$$

Then, using spatial averaging theorems for unity gives

$$\begin{aligned} -\nabla\varepsilon_\omega &= \frac{1}{V}\int_{S_{\omega\gamma}}\mathbf{n}_{\omega\gamma}dS + \frac{1}{V}\int_{S_{\omega\sigma}}\mathbf{n}_{\omega\sigma}dS \\ -\nabla\varepsilon_\gamma &= \frac{1}{V}\int_{S_{\gamma\omega}}\mathbf{n}_{\gamma\omega}dS + \frac{1}{V}\int_{S_{\gamma\sigma}}\mathbf{n}_{\gamma\sigma}dS \end{aligned} \tag{117}$$

So that we can write

$$\frac{\partial\langle c\rangle^{\gamma\omega}}{\partial t} + \nabla\cdot\ \frac{\varepsilon_\gamma}{\varepsilon_\gamma+\varepsilon_\omega}\langle c\rangle^{\gamma\omega}\left\langle\mathbf{v}_\gamma\right\rangle^\gamma\Big) = \nabla\cdot\left\{\ \frac{\varepsilon_\omega}{\varepsilon_\gamma+\varepsilon_\omega}\mathbf{D}_\omega + \frac{\varepsilon_\gamma}{\varepsilon_\gamma+\varepsilon_\omega}\mathbf{D}_\gamma\right)\cdot\nabla\langle c\rangle^{\gamma\omega}\right\} + \nabla\cdot\ \frac{\varepsilon_\omega}{\varepsilon_\gamma+\varepsilon_\omega}\mathbf{D}_\omega\cdot\nabla\langle\hat{c}_\omega\rangle^\omega + \frac{\varepsilon_\gamma}{\varepsilon_\gamma+\varepsilon_\omega}\mathbf{D}_\gamma\nabla\left\langle\hat{c}_\gamma\right\rangle^\gamma\Big) + \nabla\cdot\left\{\frac{\varepsilon_\omega}{\varepsilon_\gamma+\varepsilon_\omega}\mathbf{D}_\omega\cdot\ \frac{1}{V_\omega}\int_{S_{\omega\gamma}}\mathbf{n}_{\omega\gamma}\hat{c}_\omega dS + \frac{1}{V_\gamma}\int_{S_{\omega\sigma}}\mathbf{n}_{\omega\sigma}\hat{c}_\omega dS\right)\right\} + \nabla\cdot\left\{\frac{\varepsilon_\gamma}{\varepsilon_\gamma+\varepsilon_\omega}\mathbf{D}_\gamma\cdot\ \frac{1}{V_\gamma}\int_{S_{\gamma\omega}}\mathbf{n}_{\gamma\omega}\hat{c}_\gamma dS + \frac{1}{V_\gamma}\int_{S_{\gamma\sigma}}\mathbf{n}_{\gamma\sigma}\hat{c}_\gamma dS\right)\right\} + \nabla\cdot\ \frac{1}{\varepsilon_\gamma+\varepsilon_\omega}\mathbf{D}_\omega\cdot\nabla\varepsilon_\omega\langle\hat{c}_\omega\rangle^\omega\Big) + \nabla\cdot\ \frac{1}{\varepsilon_\gamma+\varepsilon_\omega}\mathbf{D}_\gamma\cdot\nabla\varepsilon_\gamma\left\langle\hat{c}_\gamma\right\rangle^\gamma\Big) + \frac{\varepsilon_\omega}{\varepsilon_\gamma+\varepsilon_\omega}\langle\mathcal{R}_\omega\rangle^\omega - \frac{1}{\varepsilon_\gamma+\varepsilon_\omega}\nabla\cdot\left\langle\hat{c}_\gamma\mathbf{v}_\gamma\right\rangle. \tag{118}$$

References

[1] Meunier AD, Williamson KJ. Packed bed biofilm reactors: simplified model. J Environ Eng Division 1981;107(2):307–17.
[2] Rittmann BE, McCarty PL. Model of steady-state-biofilm kinetics. Biotechnol Bioeng 1980;22(11):2343–57.
[3] Williamson K, McCarty PL. A model of substrate utilization by bacterial films. J Water Pollut Control Fed 1976;48(1):9–24.
[4] Williamson K, McCarty PL. Verification studies of the biofilm model for bacterial substrate utilization. J Water Pollut Control Fed 1976;48(2):281–96.
[5] Young JC, McCarty PL. The anaerobic filter for waste treatment, vol. 41. Water Pollution Control Federation; 1969, May. [PMID: 5791941].
[6] Singh R, Paul D, Jain RK. Biofilms: implications in bioremediation. Trends Microbiol September 2006;14(9):389–97.
[7] Scow KM, Hicks KA. Natural attenuation and enhanced bioremediation of organic contaminants in groundwater. Curr Opin Biotechnol 2005;16(3):246–53.
[8] White DC, Flemming CA, Leung KT, Macnaughton SJ. In situ microbial ecology for quantitative appraisal, monitoring, and risk assessment of pollution remediation in soils, the subsurface, the rhizosphere and in biofilms. J Microbiol Meth 1998;32(2):93–105.
[9] Field JA, Stams AJM, Kato M, Schraa G. Enhanced biodegradation of aromatic pollutants in cocultures of anaerobic and aerobic bacterial consortia. Antonie Leeuwenhoek 1995;67(1):47–77.
[10] Chen Y-M, Abriola LM, Alvarez PJJ, Anid PJ, Vogel TM. Modeling transport and biodegradation of benzene and toluene in sandy aquifer material: comparisons with experimental measurements. Water Resour Res 1992;28(7):1833–47.
[11] Borden RC, Bedient PB. Transport of dissolved hydrocarbons influenced by oxygen-limited biodegradation 1. Theoretical development. Water Resour Res 1986;22(13):1973–82.
[12] Borden RC, Bedient PB, Lee MD, Ward CH, Wilson JT. Transport of dissolved hydrocarbons influenced by oxygen-limited biodegradation 2. Field application. Water Resour Res 1986;22(13):1983–90.
[13] Mitchell AC, Phillips AJ, Hiebert R, Gerlach R, Spangler LH, Cunningham AB. Biofilm enhanced geologic sequestration of supercritical CO_2. Int J Greenhouse Gas Control 2009;3(1):90–9.
[14] Cunningham AB, Gerlach R, Spangler L, Mitchell AC. Microbially enhanced geologic containment of sequestred supercritical CO_2. Energy Procedia 2009;1(1):3245–52.
[15] de Blanc P, McKinney D, Speitel G. Advances in porous media, vol. 3. Elsevier; 1996.
[16] Murphy EM, Ginn TR. Modeling microbial processes in porous media. Hydrogeol J 2000;8:142–58.
[17] Wood BD, Whitaker S. Diffusion and reaction in biofilms. Chem Eng Sci February 1998;53(3):397–425.
[18] Picioreanu C, Van Loosdrecht MCM, Heijnen JJ. Effect of diffusive and convective substrate transport on biofilm structure formation: a two-dimensional modeling study. Biotechnol Bioeng 2000;69(5):504–15.
[19] Wood BD, Whitaker S. Multi-species diffusion and reaction in biofilms and cellular media. Chem Eng Sci September 2000;55(17):3397–418.
[20] Molz FJ, Widdowson MA, Benefield LD. Simulation of microbial growth dynamics coupled to nutrient and oxygen transport in porous media. Water Resour Res 1986;22(8):1207–16.
[21] Cunningham JA, Mendoza-Sanchez I. Equivalence of two models for biodegradation during contaminant transport in groundwater. Water Resour Res 2006;42:W02416.
[22] Rittmann BE, McCarty PL. Environmental biotechnology: principles and applications. New York: McGraw-Hill; 2001.
[23] Rittmann BE. The significance of biofilms in porous media. Water Resour Res 1993;29(7):2195–202.
[24] Baveye P, Valocchi A. An evaluation of mathematical models of the transport of biologically reacting solutes in saturated soils and aquifers. Water Resour Res 1989;25(6):1413–21.
[25] Wood BD, Quintard M, Whitaker S. Calculation of effective diffusivities for biofilms and tissues. Biotechnol Bioeng 2002;77(5):495–516.
[26] Golfier F, Wood BD, Orgogozo L, Quintard M, Buès M. Biofilms in porous media: development of macroscopic transport equations via volume averaging with closure for local mass equilibrium conditions. Adv Water Resour 2009;32(3):463–85.
[27] Whitaker S. The method of volume averaging. Kluwer Academic Publishers; 1999.
[28] Orgogozo L, Golfier F, Buès M, Quintard M. Upscaling of transport processes in porous media with biofilms in non-equilibrium conditions. Adv Water Resour 2010;33(5):585–600.
[29] Cortis A, Birkholzer J. Continuous time random walk analysis of solute transport in fractured porous media. Water Resour Res 2008;44:W06414.
[30] Cherblanc F, Ahmadi A, Quintard M. Two-domain description of solute transport in heterogeneous porous media: comparison between theoretical predictions and numerical experiments. Adv Water Resour 2007;30(5):1127–43.
[31] Cherblanc F, Ahmadi A, Quintard M. Two-medium description of dispersion in heterogeneous porous media: calculation of macroscopic properties. Water Resour Res 2003;39(6):6-1.
[32] Ahmadi A, Quintard M, Whitaker S. Transport in chemically and mechanically heterogeneous porous media, v, two-equation model for solute transport with adsorption. Adv Water Resour 1998;22:59–86.
[33] Goltz MN, Roberts PV. Three-dimensional solutions for solute transport in an infinite medium with mobile and immobile zones. Water Resour Res 1986;22(7):1139–48.
[34] Arbogast T. Derivation of the double porosity model of single phase flow via homogenization theory. SIAM J Appl Math 1985;21:3087–98.
[35] De Smedt F, Wierenga PJ. Mass transfer in porous media with immobile water. J Hydrol 1979;41:59–67.
[36] Arbogast T. The double porosity model for single phase flow in naturally fractured reservoirs. Numerical Simulation in Oil Recovery. New York: IMA Volumes in Mathematics and Its Applications. Springer Verlag; 1988.
[37] Debenest G, Quintard M. Transport in highly heterogeneous porous media: from direct simulation to macro-scale two-equation models or mixed models. Chem Prod Process Model 2008;3(1) [Article 19].
[38] Duval F, Fichot F, Quintard M. A local thermal non-equilibrium model for two-phase flows with phase-change in porous media. Int J Heat Mass Transfer 2004;47(3):613–39.
[39] Zanotti F, Carbonell RG. Development of transport equations for multiphase system-1: general development for two phase system. Chem Eng Sci 1984;39(2):263–78.
[40] Dykaar BB, Kitanidis PK. Macrotransport of a biologically reacting solute through porous media. Water Resour Res 1996;32(2):307–20.
[41] Davit Y, Quintard M, Debenest G. Equivalence between volume averaging and moments matching techniques for mass transport models in porous media. Int J Heat Mass Transfer 2010;53:4985–93.
[42] Gray WG. A derivation of the equations for multiphase transport. Chem Eng Sci 1975;30(3):229–33.
[43] Ochoa JA, Stroeve P, Whitaker S. Diffusion and reaction in cellular media. Chem Eng Sci 1986;41(12):2999–3013.
[44] Quintard M, Whitaker S. Transport in ordered and disordered porous media II: generalized volume averaging. Transp Porous Media 1994;14(2):179–206.
[45] Quintard M, Cherblanc F, Whitaker S. Dispersion in heterogeneous porous media: one-equation non-equilibrium model. Transp Porous Media 2001;44(1):181–203.
[46] Megee RD, Kinoshita S, Fredrickson AG, Tsuchiya HM. Differentiation and product formation in molds. Biotechnol Bioeng 1970, September;12(5):771–801 [PMID: 5489783].
[47] Wood BD, Whitaker S. Cellular growth in biofilms. Biotechnol Bioeng 1999;64(6):656–70.
[48] Sun Y, Lu X. A screening model for evaluating the degradation and transport of mtbe and other fuel oxygenates in groundwater. Transp Porous Media 2005;60:75–88.
[49] Chang CM, Kemblowski MW, Urroz GE. Transient stochastic analysis of biodegradable contaminant transport: first-order decay. Transp Porous Media 1999;35:1–14.
[50] Brusseau ML, Jessup RE, Rao PSC. Modeling solute transport influenced by multiprocess nonequilibrium and transformation reactions. Water Resour Res 1992;28(1):175–82.
[51] Wood BD. The role of scaling laws in upscaling. Adv Water Resour 2009;32:723–36.
[52] Golfier F, Quintard M, Whitaker S. Heat and mass transfer in tubes: an analysis using the method of volume averaging. J Porous media 2002;5(3):169–85.
[53] Ochoa-Tapia JA, Stroeve P, Whitaker S. Diffusive transport in two-phase media: spatially periodic models and Maxwell's theory for isotropic and anisotropic systems. Chem Eng Sci 1994;49:709–26.
[54] Wang J, Kitanidis PK. Analysis of macrodispersion through volume averaging: comparison with stochastic theory. Stoch Environ Res Risk Assess (SERRA) 1999;13(1):66–84.
[55] Eames I, Bush JWM. Longitudinal dispersion by bodies fixed in a potential flow. Proc Royal Soc A: Math, Phys Eng Sci 1999;455(1990):3665–86.
[56] Renard P, de Marsily G. Calculating equivalent permeability: a review. Adv Water Resour 1997;20(5–6):253–78.
[57] Pickup GE, Ringrose PS, Jensen JL, Sorbie KS. Permeability tensors for sedimentary structures. Math Geol 1994;26(2):227–50.
[58] Chrysikopoulos CV, Kitanidis PK, Roberts PV. Generalized Taylor–Aris moment analysis of the transport of sorbing solutes through porous media with spatially-periodic retardation factor. Transp Porous Media February 1992;7(2):163–85.
[59] Seymour JD, Codd SL, Gjersing EL, Stewart PS. Magnetic resonance microscopy of biofilm structure and impact on transport in a capillary bioreactor. J Magn Reson 2004;167(2):322–7.
[60] G. Iltis, R. Armstrong, D. Jansik, B. D. Wood, and D. Wildenschild. Imaging biofilm architecture within porous media using synchrotron based X-ray computed microtomography. *Submitted to Water Resources Research*, 2010.
[61] Y. Davit, G. Iltis, G. Debenest, S. Veran-Tissoires, D. Wildenschild, M. Gerino, and M. Quintard. Imaging biofilm in porous media using X-ray computed microtomography. *Accepted for publication in Journal of Microscopy*, 2010, doi:10.1111/j.1365-2818.2010.03432.x.
[62] Knutson C, Valocchi A, Werth C. Comparison of continuum and pore-scale models of nutrient biodegradation under transverse mixing conditions. Adv Water Resour 2007;30(6–7):1421–31.
[63] Shapiro M, Brenner H. Taylor dispersion of chemically reactive species: irreversible first-order reactions in bulk and on boundaries. Chem Eng Sci 1986;41:1417.
[64] Prat M. On the boundary conditions at the macroscopic level. Transp Porous Media 1989;4:259–80.
[65] Batsale J, Gobbé C, Quintard M. Local non-equilibrium heat transfer in porous media. Recent Research Developments in Heat, Mass and Momentum Transfer. Research Signpost; 1996.
[66] Valdès-Parada FJ, Goyeau B, Ochoa-Tapia JA. Diffusive mass transfer between a microporous medium and an homogeneous fluid: jump boundary conditions. Chem Eng Sci 2006;61:1692–704.

[67] Chandesris M, Jamet D. Boundary conditions at a planar fluid–porous interface for a poiseuille flow. Int J Heat Mass Transfer 2006;49:2137–50.
[68] Moyne C, Didierjean S, Amaral Souto HP, da Silveira OT. Thermal dispersion in porous media: one-equation model. Int J Heat Mass Transfer 2000;43:3853–67.
[69] Whitaker S. Introduction to fluid mechanics. Malabar, FL, USA: R.E. Krieger; 1981.
[70] Howes FA, Whitaker S. The spatial averaging theorem revisited. Chem Eng Sci 1985;40(8):1387–92.
[71] Gray WG, Leijnse A, Kolar RL, Blain CA. Mathematical tools for changing spatial scales in the analysis of physical systems. Boca Raton, FL: CRC Press; 1993.